

Renormalization Group Flow and Equation of State of Quarks and Mesons

Bernd–Jochen Schaefer *

*Institut für Kernphysik
Technische Universität Darmstadt
D-64289 Darmstadt*

and

Hans–Jürgen Pirner †

*Institut für Theoretische Physik
Universität Heidelberg
Philosophenweg 19
69120 Heidelberg, Germany*

June 22, 2021

Abstract

Nonperturbative flow equations within an effective linear sigma model coupled to constituent quarks for two quark flavors are derived and solved. A heat kernel regularization is employed for a renormalization group improved effective potential. We determine the initial values of the coupling constants in the effective potential at zero temperature. Solving the evolution equations with the same initial values at finite temperature in the chiral limit, we find a second order phase transition at $T_c \approx 150$ MeV. Due to the smooth decoupling of massive modes, we can directly link the low-temperature four-dimensional theory to the three-dimensional high-temperature theory. We calculate the equation of state in the chiral limit and for finite pion masses and determine universal critical exponents.

*Email: Schaefer@NHC.tu-darmstadt.de

†Email: pir@dxnhd1.mpi-hd.mpg.de

1 Introduction

At zero temperature and zero chemical potential, the chiral symmetry of Quantum Chromodynamics (QCD) is spontaneously broken. One expects that the chiral symmetry will be restored at sufficiently high temperature and a phase transition occurs separating the low temperature and high temperature regions. This phenomenon may be realized in high energy heavy-ion collisions at RHIC (Brookhaven) and LHC (Geneva) and is therefore a subject of general interest. It is a matter of intense debate at what temperatures the phase transition would occur and what its nature is.

In this paper we study the chiral phase transition at finite temperature both in the chiral limit and for finite pion masses. We present flow equations which link the universal critical behaviour at finite temperature to the well known physics at $T = 0$. Calculating the effective potential in the framework of the renormalization group theory with a heat kernel regularization, we investigate the critical behaviour of the chiral phase transition for two light quark flavors and calculate the critical exponents. It is still an open question whether full QCD with two massless quarks¹ and the three-dimensional $O(4)$ Heisenberg model belong to the same universality class. We use the linear sigma model with quarks which at $T = 0$ exhibits a spontaneous breaking of the $O(4)$ symmetry to an $O(3)$ symmetry. We show how the $O(4)$ symmetry is restored at sufficiently high temperature. Lattice investigations hint that the two flavor chiral phase transition lies in the $O(4)$ universality class [1] from which the behaviour of the condensates and the long distance properties at the critical temperature ensue. If this is confirmed the transition would be basically driven by the pions and the chiral sigma particle.

It was realized that a perturbative expansion of the effective potential breaks down near the critical temperature due to infrared divergences and the nature of the phase transition cannot be investigated in any finite order in perturbation theory. The situation was partly resolved in [2] by means of the average potential which employs renormalization group ideas. Constructing evolution equations for the dependence of the effective potential on a variable infrared cutoff this approach sums effectively the relevant class of perturbative diagrams in the complicated infrared regime. We follow this method and calculate in a nonperturbative way the effective potential using a variable heat kernel cutoff. The advantage of this cutoff method is that the evolution equations can be obtained in analytical form which makes the physics content very transparent. The aim of this paper is twofold: We demonstrate how the renormalization group improvement of the mass and coupling constant evolution give the main physics of the chiral phase transition, i. e. the equation of state away from the critical temperature. At low temperatures one sees the success of the model handling the pion and sigma degrees of freedom in a comparable accuracy to chiral perturbation theory. At intermediate temperatures the quarks take over as main agents contributing significantly to the change of the chiral condensate. The high temperature behavior of the linear sigma model has not enough degrees of freedom to model full QCD lacking in particular gluons.

By explicitly constructing the thermodynamic equation of state we think a more realistic assessment of the contents of the model is possible. We also think that our

¹The influence of the strange quark is neglected in this work.

method is very pedagogical making this powerful method available to physicists who are interested in an intuitive access to an otherwise very technical subject.

The paper is organized as follows: In section 2 a general summary of our formalism for an N -component ϕ^4 theory coupled to N_f quarks is given. After the calculation of the effective potential our ansatz for renormalization group improvement is presented. In section 3 the nature of the chiral phase transition is elucidated. The critical behaviour is discussed and critical exponents are determined. In this section the free energy density i.e. the thermodynamic potential for the transition and the equation of state is calculated in the chiral limit. Section 4 is reserved for a discussion of the same properties for finite pion mass. Section 5 presents our conclusions. In order to improve the readability of this paper we postpone extensive equations to appendices.

2 Flow Equations

Wilson's original renormalization group ideas have been used widely in perturbative and nonperturbative calculations. A nonperturbative approach has been used on lattices and also implemented in continuum Quantum Field Theory by Wegner, Houghton and Polchinski [3],[4]. Flow equations describe the average of an effective action over a volume and are the continuum analogue of a block spin transformation on the lattice. All degrees of freedom with momenta larger than an infrared scale k , the coarse graining scale, are effectively integrated out. The flow equations are ultraviolet and infrared finite through the introduction of an infrared cutoff function f_k , which obeys several requirements described in the next subsection. The solution of these equations provides the full effective potential, once the infrared cutoff k is removed ($k \rightarrow 0$). On the other side in the limit $k \rightarrow \infty$ or k equal to some ultraviolet cutoff Λ the effective average potential results in the classical potential where no fluctuations are included. This ultraviolet cutoff may be associated with the highest momentum scale for which the theory parameterizes the physics adequately. All quantum fluctuations with momenta larger than Λ are included in the potential at this scale, thus no further necessity for an ultraviolet regularization scheme arises. The effective couplings at the large scale Λ specify the potential completely. The knowledge of the k -dependence of the effective average potential then allows to interpolate from the classical 'bare' potential at $k = \Lambda$ down to the effective 'renormalized' potential for $k \rightarrow 0$ including more and more quantum fluctuations as the evolution proceeds towards zero.

This method of the flow equation has been developed intensively by Wetterich and his collaborators [2]. One important ingredient of the evolution equation approach by this group is the appearance of the exact inverse propagator in the flow equation, which makes the RG-improved one-loop equation exact and intrinsically complicated [21]. The solved truncation of this exact equation is very similar to the RG-improved one loop equations used here where the bare couplings are replaced by their corresponding full k -dependent expressions. The technically difficult part in the exact RG-approach is not the establishment of an exact relation, but rather the choice of a suitable nonperturbative truncation scheme in order to solve this highly nonlinear coupled set of differential equations. We use a simple truncation scheme

and analytical flow equations can be derived. We believe that a deeper connection between Wetterich's and our approach should be possible.

The flow equations are nonperturbative, i.e. also applicable for problems with large couplings, loosely spoken, because the evolution of the different couplings is interlinked and no particular truncation in coupling constant is used. The solutions of the flow equations give an accurate picture of the high temperature phase transition in four dimensions. It is possible to study the phase transition at the critical temperature and to calculate the critical exponents with surprisingly high accuracy.

2.1 The Effective Potential

In this subsection we develop the formalism starting with the derivation of the flow equations for the linear $SU(2) \times SU(2)$ sigma model combined with two quark flavours. The linear sigma model is a hybrid model which contains quark and mesonic σ - and π -fields as collective degrees of freedom in order to simplify the strong $q\bar{q}$ interaction. The cutoff Λ plays the role of a compositeness scale, below which the effective σ - and π -fields can be treated as elementary. For the moment we leave the connection of this theory to QCD as an open question and see how far we get with this model. Preliminary investigations in this direction have been made in ref. [6].

The partition function at zero temperature is given by

$$Z[J = 0] = \int \mathcal{D}q \mathcal{D}\bar{q} \mathcal{D}\sigma \mathcal{D}\vec{\pi} \exp\left\{- \int d^4x (\mathcal{L}_F + \mathcal{L}_B)\right\} . \quad (1)$$

Here we omit any external sources J , because in the one loop approximation the effective potential and the generating functional for one particle irreducible Green functions do not differ. The Euclidean² Lagrangian in $d = 4$ dimensions looks like

$$\mathcal{L}_F = \bar{q}(x) (\gamma_E \partial_E + g(\sigma + i\vec{\tau}\vec{\pi}\gamma_5)) q(x) , \quad (2)$$

$$\mathcal{L}_B = \frac{1}{2} \left((\partial_\mu \sigma)^2 + (\partial_\mu \vec{\pi})^2 \right) + \frac{m_0^2}{2} (\sigma^2 + \vec{\pi}^2) + \frac{\lambda_0}{4} (\sigma^2 + \vec{\pi}^2)^2 - c\sigma . \quad (3)$$

The parameter c is an explicit symmetry breaking term in σ -direction, which gives the Goldstone boson a finite mass. In order to avoid later any recurrences we derive the effective potential with an explicit symmetry breaking term c . The chiral limit can be extracted by putting c to zero in all equations.

Taking advantage of the properties of the minimum ϕ_0 of the potential we can eliminate the mass parameter m_0^2 in favour of λ_0 and ϕ_0 . Then the potential can be written with $m_0^2 = c/\phi_0 - \lambda_0\phi_0^2$ as

$$V = \frac{\lambda_0}{4} \left(\vec{\phi}^2 - \phi_0^2 \right)^2 - \frac{\lambda_0}{4} \phi_0^4 - c \left(\sigma - \frac{\vec{\phi}^2}{2\phi_0} \right) \quad (4)$$

where we introduce the $O(4)$ vector $\vec{\phi} = (\sigma, \vec{\pi})$ as a shorthand notation for the meson fields.

²We denote all Euclidean operators with an index 'E'.

Formal integration over the fermions yields a non-local determinant, which can be regularized by the heat kernel representation. We use the abbreviations $M(x) = \sigma(x) + i\vec{\tau}\vec{\pi}(x)\gamma_5$, ($MM^+ = \vec{\phi}^2$) and $D = \gamma_E\partial_E + gM(x)$.

$$\begin{aligned}
Z[J=0] &= \int \mathcal{D}\sigma\mathcal{D}\vec{\pi} \det(\gamma_E\partial_E + gM(x)) \exp\{-\int d^4x\mathcal{L}_B\} \\
&= \int \mathcal{D}\sigma\mathcal{D}\vec{\pi} \exp\{\frac{1}{2}\text{Tr} \log DD^+ - \int d^4x\mathcal{L}_B\} \\
&= \int \mathcal{D}\sigma\mathcal{D}\vec{\pi} \exp\{-\int d^4x\mathcal{L}_B + \\
&\quad -\frac{1}{2}\int_{1/\Lambda^2}^{\infty} \frac{d\tau}{\tau} \int d^4x \text{tr}\langle x|e^{-\tau(-\partial_E^2+g^2MM^++g\gamma\cdot\partial M^+)}|x\rangle\} \quad .
\end{aligned} \tag{5}$$

We remark that the lower boundary of the integral over the proper time τ reflects the ultraviolet cutoff scale Λ , while the upper limit of the proper time integral represents the infrared scale. Later, we will choose an infrared cutoff function in such a way that no ultraviolet cutoff in the proper time integration is needed. Details concerning the heat kernel representation and definitions can be found in ref. [12].

Because we are interested in the calculation of the effective potential no wave function renormalization corrections are taken into account. This means that we set the wave function renormalization constant $Z_k = 1$, which simplifies further calculations because derivatives resulting from the heat kernel expression can be omitted. This is not a principal restriction of the method. On the contrary the chosen heat kernel regularization is designed for a derivative expansion and higher derivatives can be taken into account not only for flat manifolds but also for curved manifolds [5].

We find for the partition function at zero temperature the following expression which is exact up to the omission of derivatives $\partial_\mu\phi$ in the fermion exponent

$$Z[J=0] = \int \mathcal{D}\sigma\mathcal{D}\vec{\pi} \exp\{-\frac{1}{2}\int_{1/\Lambda^2}^{\infty} \frac{d\tau}{\tau} \int d^4x \text{tr}\langle x|e^{-\tau(-\partial_E^2+g^2\vec{\phi}^2)}|x\rangle - \int d^4x\mathcal{L}_B\} \quad . \tag{6}$$

The fermion determinant is in general part of the functional integration over the remaining meson fields weighted by the meson Lagrangian \mathcal{L}_B . In the following we limit this integration over the fermions to the one-loop level. Thus we decouple the effect of modified fermions back on the meson dynamics, pull the non-local determinant in front of the meson integration and replace the meson fields $\vec{\phi}^2$ with the vacuum expectation value (VEV) ϕ_0^2 . The total effective action splits into two pieces and becomes a sum of fermionic and bosonic terms each depending on ϕ_0 :

$$-\ln Z = \Gamma(\phi_0) = \Gamma^F(\phi_0) + \Gamma^B(\phi_0). \tag{7}$$

In a plane wave basis for the diagonal part of the heat kernel [12] the effective action for the fermions Γ^F has the form

$$\Gamma^F(\phi_0) = \frac{1}{2} \int d^4x \int_{1/\Lambda^2}^{\infty} \frac{d\tau}{\tau} \int \frac{d^4q}{(2\pi)^4} \left\{ \text{tr}_{N_c N_f \gamma} e^{-\tau(q^2+g^2\phi_0^2)} \right\} \quad , \tag{8}$$

where the trace runs over color-, flavor- and spin-space and gives a factor $8N_c$ for two quark flavours.

The remaining meson integration is also performed on a one loop level and is obtained by a saddle point approximation. The classical mesonic potential $V_0 = m_0^2 \vec{\phi}^2/2 + \lambda_0 (\vec{\phi}^2)^2/4 - c\sigma$ is expanded around the minimum, which corresponds to the VEV ϕ_0 . Thus taking quadratic fluctuations of the mesons into account and using again a heat kernel regularization for the fluctuation determinant one finds the effective action for the bosons:

$$\Gamma^B(\phi_0) = -\frac{1}{2} \int d^4x \int_{1/\Lambda^2}^{\infty} \frac{d\tau}{\tau} \int \frac{d^4q}{(2\pi)^4} \left\{ \text{tr}_N e^{-\tau(q^2 + \frac{\partial^2 V_0}{\partial \phi_i \partial \phi_j})} \right\} . \quad (9)$$

Here the trace runs over the (4×4) fluctuation matrices in $(\sigma, \vec{\pi})$ -space. Note the opposite sign of the bosonic and fermionic effective actions. In the σ -model the calculation of the second derivatives of the potential V_0 is straightforward and the trace can be evaluated explicitly for $N(= 4)$ components. One has to determine the eigenvalues of the fluctuation matrix evaluated at the minimum of the potential i. e. the masses of the system. With an explicit symmetry breaking term c the trace is given by

$$\text{tr}_N e^{-\tau \frac{\partial^2 V_0}{\partial \phi_i \partial \phi_j}} \Big|_{\vec{\phi}^2 = \phi_0^2} = 3e^{-\tau c/\phi_0} + e^{-\tau(2\lambda_0 \phi_0^2 + c/\phi_0)} . \quad (10)$$

The first term on the r.h.s. of eq. (10) represents the mass squared eigenvalues associated with the three pions while the other term describes the σ -meson (cf. eqs. (59)-(61)). In general this trace is a sum over all exponentiated squares of mass eigenvalues times the proper time τ .

2.2 The Renormalization Group Improvement

The effective action $\Gamma(\phi_0)$, eqs. (7)-(9), contains so far only fluctuations up to the one loop level and depends on the ultraviolet heat kernel cutoff Λ via the proper time integration. In order to cut off the fluctuations in the infrared we introduce into the proper time integrand a universal k -dependent function

$$f_k(\tau) = g(x) \quad (11)$$

$$x = \tau k^2 \quad (12)$$

with a dimensionless argument $x = \tau k^2$ which depends on the product of the proper time and the square of the infrared cutoff k . This function f_k has to satisfy three conditions:

We require that $g(x \rightarrow 0) = f_k(\tau k^2 \rightarrow 0) = 1$, since the action Γ_k with infrared cutoff should tend to the full effective action Γ at $k = 0$, i. e. in the limit $k \rightarrow 0$ the infrared cutoff is removed.

The function g must satisfy $g(x \rightarrow \infty) \rightarrow 0$, to suppress modes with fixed ‘‘virtuality’’ k for large τ . Remember that the upper limit of the proper time integration represents the infrared regime of the effective action which is regularized by this condition of the function g .

Thirdly, the first derivative of the cutoff function g has to obey

$$g'(x) = -x^2 h(x) \quad (13)$$

with $h(x)$ being any regular function in the vicinity of the origin. This condition assures that the renormalization group equations for the k -dependent effective action are ultraviolet finite. The cutoff function regularizes the derivative of the effective potential with respect to the infrared parameter k , therefore a further ultraviolet heat kernel cutoff Λ is unwanted. Due the above condition the ultraviolet divergences in the effective action itself are not affected by the presence of the infrared cutoff [21, 25]. It is this condition which distinguishes the cutoff function from a simple minded mass cutoff.

One possible choice for the function $g(x)$ which satisfy all these requirements is

$$g(x) = e^{-x} \left(1 + x + \frac{1}{2}x^2 \right) \quad (14)$$

The function g depicts a smooth cutoff of the momentum modes and allows for an elegant and simple form of the evolution equations.

A smooth cutoff is unavoidable if one wants to have a well defined derivative expansion. For the effective potential alone also a sharp cutoff would do [4],[9],[8].

Even in this case the above choice has great advantages over a sharp cutoff, at least in the proper-time integral formalism where it may cause unpleasant oscillations (cf. e.g.[28]).

The effective action with the cutoff function $f_k(\tau)$ has now the following form:

$$\Gamma_k[\phi_0] = \int d^4x V_k(\phi_0) \quad (15)$$

with

$$V_k = -\frac{1}{2} \int_0^\infty \frac{d\tau}{\tau} f_k(\tau) \int \frac{d^4q}{(2\pi)^4} \left\{ tr_N e^{-\tau(q^2 + \frac{\partial^2 V_0}{\partial \phi_i \partial \phi_j})} - tr e^{-\tau(q^2 + g^2 \tilde{\phi}^2)} \right\} . \quad (16)$$

This equation defines the one loop effective potential with an additional infrared cutoff function. In a further approximation we truncate the effective potential at terms $\propto (\tilde{\phi}^2)^2$. Such a procedure leads to simple evolution differential equations for few couplings (λ, m^2) . These evolution equations are improved by replacing the bare couplings (λ_0, m_0^2) and the constant VEV (ϕ_0) with the running couplings (λ_k, m_k^2) and the running VEV (ϕ_k) . This renormalization group improvement resums the relevant infrared divergent Feynman diagrams and gives the important nonperturbative evolution of the potential. The substitution can be compared with ordinary renormalization of n -point functions in perturbation theory, where one replaces on the one loop level the bare couplings with the renormalized ones. This simple strategy is pursued in this paper and has many advantages. Another possibility is to derive an evolution equation for the full potential using the heat kernel regularization. This is postponed to another paper in the future [16].

The evolution of the potential itself with virtuality k leads to two phases and therefore two sets of equations. In the chiral limit the minimum of the potential (VEV) will evolve from a large value to zero in a second order phase transition. For finite pion masses ($c \neq 0$) this transition becomes a crossover and the two sets of flow equations merge to one set of equations, as we will show analytically. In order to simplify and clarify the following discussion we start with the chiral limit and set $c = 0$ for the rest of this section.

For high virtuality k the system is in the symmetric phase which is defined by a vanishing VEV ($\phi_k = 0$) of the potential. Through the derivative with respect to the fields

$$V'_k := \frac{\partial V_k}{\partial \phi^2} \quad (17)$$

we can define the mass m_k^2 and the coupling constant λ_k in the symmetric regime

$$\begin{aligned} \frac{m_k^2}{2} &:= V'_k(\vec{\phi}^2 = \phi_k^2 = 0) \quad , \\ \frac{\lambda_k}{2} &:= V''_k(\vec{\phi}^2 = \phi_k^2 = 0) \quad . \end{aligned} \quad (18)$$

The effective potential at the minimum is given by

$$v_k := V_k(\vec{\phi}^2 = \phi_k^2 = 0) \quad . \quad (19)$$

Taking the derivatives of equation (16) with respect to the scale k we find the following coupled sets of flow equations for the symmetric phase ($\phi_k^2 = 0$):

$$k \frac{\partial v_k}{\partial k} = k \frac{\partial V_k(0)}{\partial k} \quad , \quad (20)$$

$$\frac{k}{2} \frac{\partial m_k^2}{\partial k} = k \frac{\partial V'_k(0)}{\partial k} \quad , \quad (21)$$

$$\frac{k}{2} \frac{\partial \lambda_k}{\partial k} = k \frac{\partial V''_k(0)}{\partial k} \quad . \quad (22)$$

In the spontaneously broken region the VEV is finite ($\phi_k \neq 0$) and the mass parameter m_k^2 tends to negative values. We prefer to parameterize the evolution of the potential in this region in terms of λ_k and the minimum of the potential ϕ_k , which is defined by

$$V'_k(\phi_k) = 0 \quad . \quad (23)$$

This equation enables us to find the evolution of the minimum ϕ_k . By again taking the derivatives with respect to the scale k we find the flow equation for ϕ_k^2 in the broken phase ($\phi_k^2 \neq 0$)

$$k \frac{\partial v_k}{\partial k} = k \frac{\partial V_k(\phi_k^2)}{\partial k} \quad , \quad (24)$$

$$\frac{k}{2} \frac{\partial \phi_k^2}{\partial k} = -\frac{k}{2V''_k(\phi_k^2)} \frac{\partial V'_k(\phi_k^2)}{\partial k} = -\frac{k}{\lambda_k} \frac{\partial V'_k(\phi_k^2)}{\partial k} \quad , \quad (25)$$

$$\frac{k}{2} \frac{\partial \lambda_k}{\partial k} = k \frac{\partial V''_k(\phi_k^2)}{\partial k} \quad , \quad \text{if } V'''_k = 0 \quad . \quad (26)$$

Here an important remark must be added, that we first evaluate the derivatives on the right hand sides for constant couplings λ_0 , m_0^2 and constant VEV ϕ_0 with respect to k . Thus the scale derivative acts only on the infrared cutoff function $f_k(\tau)$ inside the proper time integrand.

3 Equation of state in the chiral limit

In this section we discuss the flow equations for the two flavour linear sigma model in the chiral limit. We present the numerical solution of the flow equations with respect to the scale k and generalize the equations to finite temperature.

3.1 The evolution for $T = 0$

In the symmetric phase at zero temperature we use the equations (20,21,22) and get the evolution equations for the free energy density, mass parameter and quartic coupling. Due to the choice of the cutoff function $f_k(\tau)$ the resulting equations are very transparent. The heat kernel cutoff is not a simple mass cutoff, in effect the derivative cf. eq. (14) of the cutoff function is simpler than the cutoff function itself, therefore the evolution equations have such a concise form:

$$k \frac{\partial v_k}{\partial k} = -\frac{20}{2(4\pi)^2} k^4, \quad (27)$$

$$\frac{k}{2} \frac{\partial m_k^2}{\partial k} = -\frac{3\lambda_k k^2}{(4\pi)^2} \frac{1}{(1 + m_k^2/k^2)^2} + \frac{4N_c g^2 k^2}{(4\pi)^2}, \quad (28)$$

$$\frac{k}{2} \frac{\partial \lambda_k}{\partial k} = \frac{12\lambda_k^2}{(4\pi)^2} \frac{1}{(1 + m_k^2/k^2)^3} - \frac{8N_c g^4}{(4\pi)^2}. \quad (29)$$

The factor 20 in eq. (27) arises from the combination $4 - 8N_c$ (4 mesons minus $4N_f N_c = 8N_c$ fermionic degrees of freedom). In the symmetric phase the pions are degenerate with the σ -meson and the squared mass parameter is always positive. The VEV ϕ_k vanishes and does not appear on the right hand sides of the evolution equations. In the broken phase the pion mass vanishes in the chiral limit. The constituent quark mass is proportional to $g\phi_k$ and is zero in the symmetric phase.

To solve the evolution equations we need three initial values of v_k , λ_k and m_k^2 at $k = \Lambda$ in the UV. We start the evolution in the symmetric phase deep in the ultraviolet region of QCD at $\Lambda = 1.2$ GeV and set $v_k = 0$. The other two parameters λ_k and m_k^2 are adjusted to get $\phi_{k=0} = 93\text{MeV} = f_\pi$ at $k = 0$ and the transition to chiral symmetry breaking at $k = k_{\chi SB} = 0.8$ GeV. This leads to $m_{k=\Lambda}^2 = (550\text{MeV})^2$ and $\lambda_{k=\Lambda} = 40$.

In addition we need the Yukawa coupling g which we fix to $g = 3.2$ for all k in order to get a constituent quark mass of 300 MeV at the end of the evolution. Because we do not take any wave function renormalization into account g has only a weak scale dependence. In the work of Wetterich et al. [2] the main contribution to the strong evolution of the Yukawa coupling stems from the evolution of the meson wave function renormalization.

In fact, the initial value for the quartic coupling $\lambda_{k=\Lambda}$ turns out to be not very important due to the Gaussian fix point $\lambda(k \rightarrow 0) \rightarrow 0$. This behaviour can be seen in figure 1, where the evolution of the quartic coupling towards zero for different initial values is plotted. Near $k = \Lambda$ the evolution of λ_k is dominated by the bosonic part, the first term on the r.h.s. of eq. (29) whereas the evolution of m_k^2 responds to the fermion loops. When we reach chiral symmetry breaking at the scale

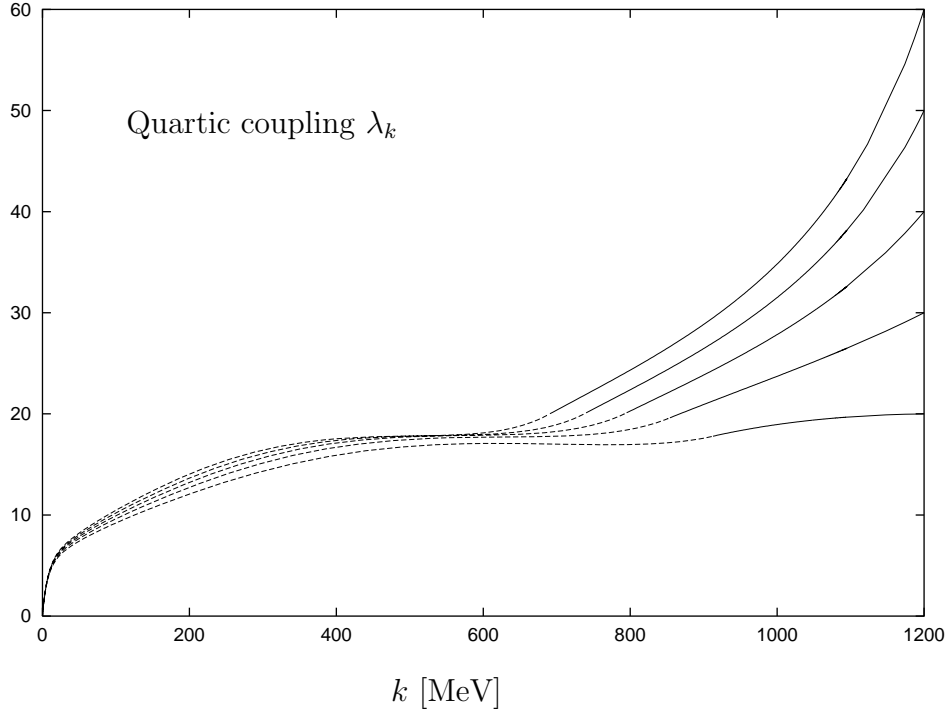


Figure 1: The evolution of λ_k with respect to the scale k for different initial values.

$k = k_{\chi SB} \approx 0.8$ GeV, we switch to the equations for the broken phase characterized by $\phi_k^2 \neq 0$:

$$k \frac{\partial v_k}{\partial k} = \frac{k^4}{2(4\pi)^2} \left[3 + \frac{1}{(1 + 2\lambda_k \phi_k^2/k^2)} - \frac{8N_c}{(1 + g^2 \phi_k^2/k^2)} \right], \quad (30)$$

$$\frac{k}{2} \frac{\partial \phi_k^2}{\partial k} = \frac{3k^2}{2(4\pi)^2} \left[1 + \frac{1}{(1 + 2\lambda_k \phi_k^2/k^2)^2} \right] - \frac{4N_c}{(4\pi)^2} \frac{k^2 g^2}{\lambda_k} \left[\frac{1}{(1 + g^2 \phi_k^2/k^2)^2} \right], \quad (31)$$

$$\frac{k}{2} \frac{\partial \lambda_k}{\partial k} = \frac{3\lambda_k^2}{(4\pi)^2} \left[1 + \frac{3}{(1 + 2\lambda_k \phi_k^2/k^2)^3} \right] - \frac{8N_c}{(4\pi)^2} g^4 \left[\frac{1}{(1 + g^2 \phi_k^2/k^2)^3} \right]. \quad (32)$$

The first two terms on the r.h.s. of the above equations are again related to the boson fluctuations while the last parts are connected to the fermionic contributions to the evolution.

The constant factor in the first part of the upper equations comes from the three massless pions while the second part of the bosonic term contains the contribution of the σ -meson with squared mass $2\lambda_k \phi_k^2$. In the broken phase the σ -meson is massive ($\phi_k \neq 0$) and the σ -meson contribution decouples from the evolution for small k values in the IR region, when $k \ll 2\lambda_k \phi_k^2$; whereas the massless pions contribute permanently to the flow in the chiral limit. The fermionic quark part of the flow equation enters with the opposite sign to the evolution and the quarks become more and more massive in the infrared. The factors have a similar origin as in the symmetric phase. The contribution from the pions is three times larger than the σ -meson contribution. Two flavors, two particles and anti-particles and two spin degrees of freedom yield a factor of $8N_c$.

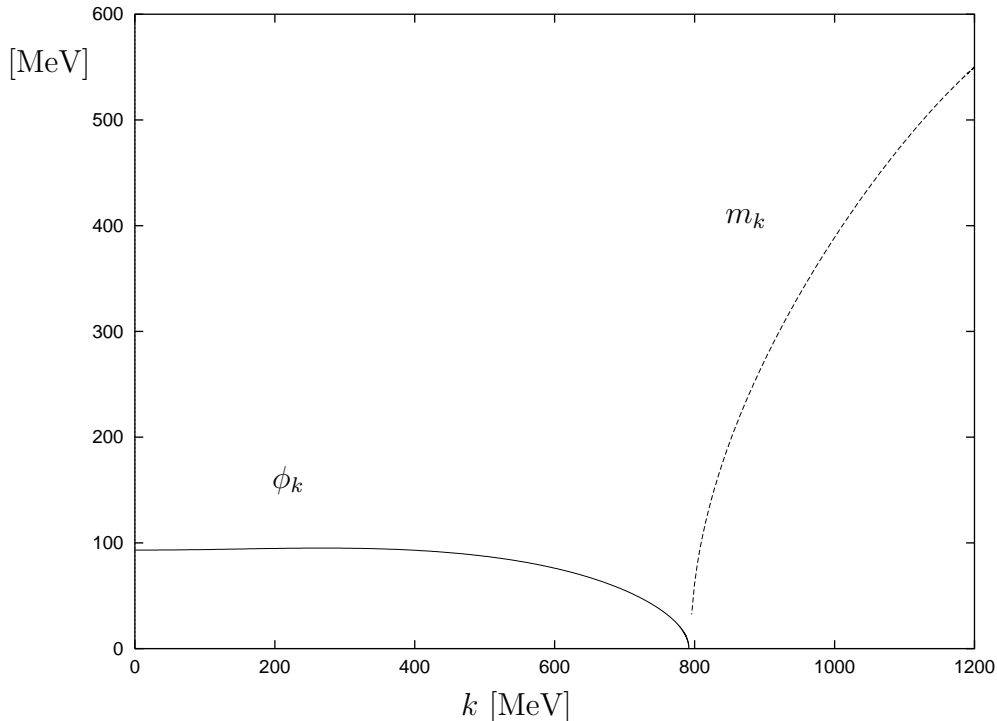


Figure 2: The evolution of the minimum of the effective potential ϕ_k for $k < k_{\chi SB}$ and the evolution of the mass parameter m_k for $k > k_{\chi SB}$.

The functions in squared brackets can be called threshold functions, because they describe the smooth decoupling of massive modes from the evolution towards the infrared limit of the theory given by the scale k . With the heat kernel method and our choice of the function $f_k(\tau)$ we can calculate these threshold functions analytically. They are of the form $(1 + \text{mass}^2/k^2)^{-p}$ where p is some positive integer power. So the quark loop gives a factor $(1 + g^2\phi_k^2/k^2)^{-p}$ with positive p which switches off the quark contribution to the evolution of the couplings for $k \ll g\phi_k$. Similarly, the square of the sigma mass over the infrared scale $2\lambda_k\phi_k^2/k^2$ suppresses the massive boson loop. At small evolution parameters only zero mass pion loops drive the evolution. This is very intuitive and coincides with the ideas of chiral perturbation theory. In fact, it has been also shown [20] that this model reproduces the chiral expansions even beyond leading order. As we will see in the equation of state the suppression of the quark terms for the evolution does not mean that the quarks do not contribute to the thermodynamic functions like the pressure or energy density below the phase transition temperature. In this respect the model has the same defects as more naive NJL models without quark confinement.

We remark that in the heat kernel expression for the effective potential the inverse fermion propagator enters quadratically in the combination DD^+ therefore we can use the same infrared cutoff function f_k as in the bosonic integral without breaking chiral symmetry. If we want to take into account the running of the Yukawa coupling g the fermion propagators also have to be squared. One also recognizes the signs of the bosonic and fermionic contributions to the β -function. The bosons lead to an infrared stable (ultraviolet unstable) λ -coupling, whereas the fermions counteract

this tendency. Going from high k to low k one sees that the mesonic self-interaction λ_k will balance at intermediate values of k , whereas in the far infrared the boson term wins (cf. figure 1). The chiral symmetry changes at $k = k_{\chi SB} \approx 800$ MeV, where the system goes over from the symmetric phase to the spontaneously broken phase. At this scale k eqs. (29) and (32) become identical, i.e. the β -function of λ_k is continuous (cf. figure 1).

We have argued in a separate paper [11] that this transition at zero temperature may be visible in electron scattering, where real photoproduction with virtuality $Q^2 = 0$ corresponds to a heat kernel cutoff $k^2 = 0$ and inelastic scattering with higher Q^2 to the equivalent k^2 scales. The transition with increasing k from the constituent quark to the parton in deep inelastic scattering is a natural consequence in the linear sigma model. The vacuum expectation value ϕ_k stabilizes at small values of k and the evolution ends with $\lim_{k \rightarrow 0} \phi_k = f_\pi$. When the heavy particles, the sigma and quarks, have decoupled, the change of the vacuum expectation value becomes proportional to k , the evolution stops (see figure 2). It is interesting to investigate how a more sophisticated calculation with running Yukawa coupling g_k and wave function renormalization Z_k relates the field theoretic model to more observables. Thereby the evolution itself may be tested in a region which perturbative QCD i. e. the Altarelli Parisi evolution equations cannot reach.

3.2 The evolution for finite T

The extension of the flow equations to finite temperature for thermal equilibrium is achieved by the Matsubara technique. We integrate the momenta in equation (16), by splitting the zero momentum component from the three-dimensional spatial momentum components and convert the integration over q_0 into a summation over Matsubara frequencies ω_n for the bosons and ν_n for the quarks [7]:

$$\omega_n^2 = 4\pi^2 n^2 T^2 \quad , \quad (33)$$

$$\nu_n^2 = (2n + 1)^2 \pi^2 T^2 \quad ; \quad n \in \mathbb{Z} \quad . \quad (34)$$

In the symmetric phase the corresponding equations are written in terms of the positive mass parameter m_k^2 and λ_k :

$$k \frac{\partial v_k}{\partial k} = \frac{k^4}{2(4\pi)^2} \frac{\pi T}{k} \left[4 \sum_{n=-\infty}^{\infty} \frac{1}{(1 + \omega_n^2/k^2)^{3/2}} - 8N_c \sum_{n=-\infty}^{\infty} \frac{1}{(1 + \nu_n^2/k^2)^{3/2}} \right], \quad (35)$$

$$\begin{aligned} \frac{k}{2} \frac{\partial m_k^2}{\partial k} &= -\frac{3\lambda_k^T}{(4\pi)^2} k^2 \left[\frac{3\pi T}{2k} \sum_{n=-\infty}^{\infty} \frac{1}{(1 + (\omega_n^2 + m_k^2)/k^2)^{5/2}} \right] \\ &+ \frac{4N_c g^2}{(4\pi)^2} k^2 \left[\frac{3\pi T}{2k} \sum_{n=-\infty}^{\infty} \frac{1}{(1 + \nu_n^2/k^2)^{5/2}} \right] \quad , \quad (36) \end{aligned}$$

$$\begin{aligned} \frac{k}{2} \frac{\partial \lambda_k^T}{\partial k} &= \frac{12(\lambda_k^T)^2}{(4\pi)^2} \left[\frac{15\pi T}{8k} \sum_{n=-\infty}^{\infty} \frac{1}{(1 + (\omega_n^2 + m_k^2)/k^2)^{7/2}} \right] \\ &- \frac{8N_c g^4}{(4\pi)^2} \left[\frac{15\pi T}{8k} \sum_{n=-\infty}^{\infty} \frac{1}{(1 + \nu_n^2/k^2)^{7/2}} \right] \quad . \quad (37) \end{aligned}$$

The flow equation for the free energy density $v_k(0)$ in the symmetric phase, eq. (35), does not depend on any coupling neither at zero nor at finite temperature. The minimum of the effective potential yields an integration constant. Each contribution to the flow equations at finite temperature is taken into account in a similar way as in the zero temperature case (see above). The modifications in the flow equations appear in the threshold functions within the squared brackets in eqs. (35) - (37).

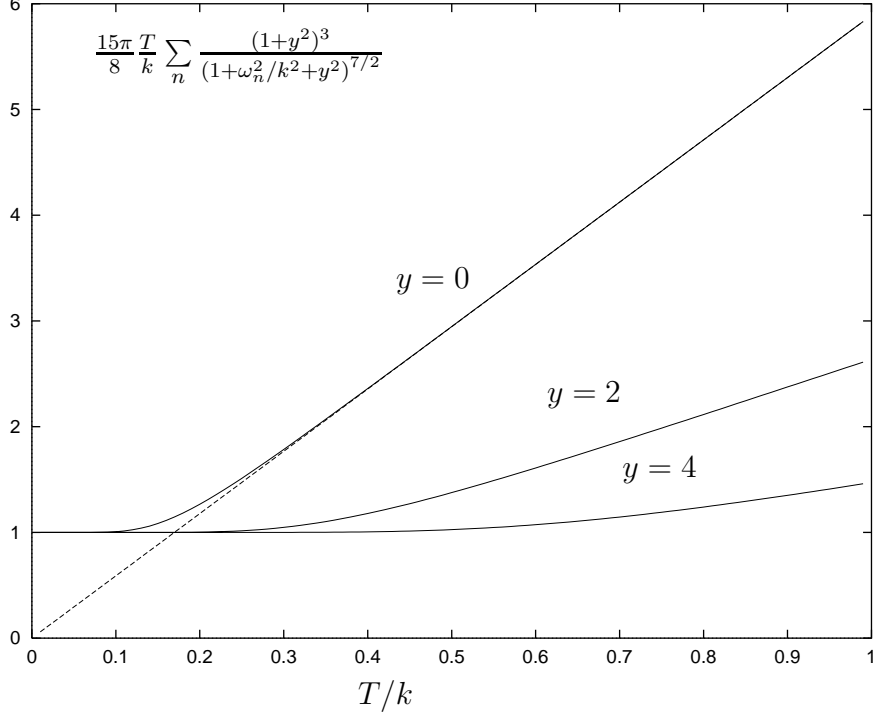


Figure 3: The ratio of bosonic threshold functions for temperature $T = 0$ and $T \neq 0$ with different mass parameters $y = 0, 2, 4$ as function of T/k . The dashed line is the function $15\pi/8 \cdot T/k$ which demonstrates the linear behaviour of the threshold function for large T/k in the case of $y = 0$.

For the broken phase we get the following expressions:

$$k \frac{\partial v_k}{\partial k} = \frac{k^4}{2(4\pi)^2} \frac{\pi T}{k} \left[3 \sum_{n=-\infty}^{\infty} \frac{1}{(1 + \omega_n^2/k^2)^{3/2}} + \sum_{n=-\infty}^{\infty} \frac{1}{(1 + (\omega_n^2 + 2\lambda_k^T(\phi_k^T)^2)/k^2)^{3/2}} - 8N_c \sum_{n=-\infty}^{\infty} \frac{1}{(1 + (\nu_n^2 + g^2(\phi_k^T)^2)/k^2)^{3/2}} \right]. \quad (38)$$

$$\frac{k}{2} \frac{\partial(\phi_k^T)^2}{\partial k} = \frac{3k^2}{2(4\pi)^2} \left[\frac{3\pi T}{2k} \sum_{n=-\infty}^{\infty} \left\{ \frac{1}{(1 + \omega_n^2/k^2)^{5/2}} + \frac{1}{(1 + (\omega_n^2 + 2\lambda_k^T(\phi_k^T)^2)/k^2)^{5/2}} \right\} - \frac{4N_c}{(4\pi)^2} \frac{g^2 k^2}{\lambda_k^T} \left[\frac{3\pi T}{2k} \sum_{n=-\infty}^{\infty} \frac{1}{(1 + (\nu_n^2 + g^2(\phi_k^T)^2)/k^2)^{5/2}} \right] \right], \quad (39)$$

$$\frac{k}{2} \frac{\partial \lambda_k^T}{\partial k} = \frac{3(\lambda_k^T)^2}{(4\pi)^2} \left[\frac{15\pi T}{8k} \sum_{n=-\infty}^{\infty} \left\{ \frac{1}{(1 + \omega_n^2/k^2)^{7/2}} + \frac{3}{(1 + (\omega_n^2 + 2\lambda_k^T(\phi_k^T)^2)/k^2)^{7/2}} \right\} \right]$$

$$-\frac{8N_c}{(4\pi)^2}g^4 \left[\frac{15\pi T}{8k} \sum_{n=-\infty}^{\infty} \frac{1}{(1 + (\nu_n^2 + g^2(\phi_k^T)^2)/k^2)^{7/2}} \right] . \quad (40)$$

In the limit $\phi_k \rightarrow 0$, i.e. at the chiral symmetry breaking scale $k_{\chi SB}$ the equations for the symmetric and the broken phase are continuous.

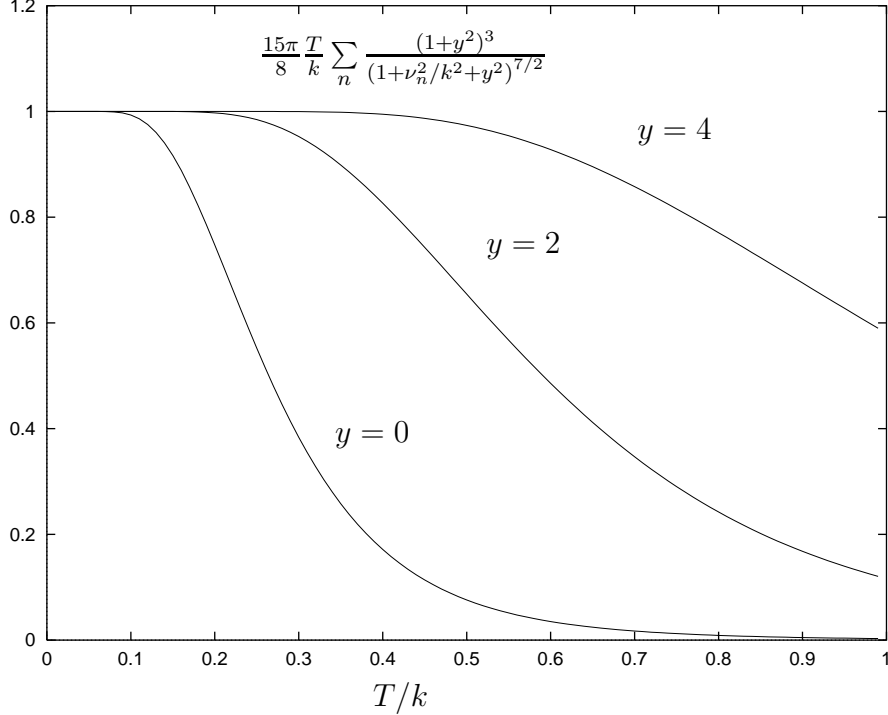


Figure 4: The ratio of fermionic threshold functions for $T = 0$ and $T \neq 0$ with different mass parameters $y = 0, 2, 4$ as function of T/k .

One sees that the equations arise from the same one loop diagrams as the $T = 0$ equations and therefore depend on the coupling constants in a similar way. Due to the three dimensional momentum integrations fractional powers arise in the threshold functions.

In the limit of low temperatures $T/k \rightarrow 0$ we regain our old expressions at $T = 0$, i.e. we have the relations:

$$\frac{3\pi T}{2k} \sum_{n=-\infty}^{\infty} \frac{1}{\left(1 + \left\{ \frac{\omega_n^2}{\nu_n^2} \right\} / k^2 + y^2\right)^{5/2}} \rightarrow \frac{1}{(1+y^2)^2} \quad (41)$$

It is possible to analytically relate all Matsubara sums to the corresponding four dimensional integrals in the low temperature limit cf. appendix A and ref. [18]. The above equations guarantee the right matching of the finite temperature equations to the zero temperature equations, i.e. in the limit $T \rightarrow 0$ the sets of equations for finite and zero temperature become identical.

We plot in figure 3 the ratios of finite temperature bosonic threshold function appearing in the β -function for λ_k^T over the zero temperature β -function for λ_k .

Figure 4 shows the equivalent ratios of threshold functions for the fermions. For small ratios T/k up to 0.1 the threshold function ratio is constant which means that for temperatures small compared to the infrared cutoff scale all Matsubara modes are important. The summation is effectively a continuous integration.

For large ratios T/k the bosonic threshold functions increase linearly in T/k . (cf. figure 3). This increase is due to the $n = 0$ Matsubara mode in the frequency sum. In the large temperature limit the (3+1)-dimensional system reduces to a 3-dimensional system. Thus the phenomenon of dimensional reduction is automatically included in the bosonic threshold functions. In the fermionic case there is no zero Matsubara frequency, therefore the fermionic threshold functions decrease with T/k and become zero. This means that for high T/k the fermions decouple from the further evolution. There also exists a stable plateau in the vicinity of the origin for the Fermi-case as in the ref. [2].

The dimensional reduction manifests itself in the critical behaviour, as will be shown in the next section.

3.3 Critical behaviour and exponents

The idea underlying the finite temperature calculation is the following: At large ultraviolet scale $k = \Lambda$ and finite temperature T the couplings of the effective theory are identical to the $T = 0$ case, since the finite temperature only modifies the boundary in the imaginary time direction but not the dynamics on a small scale in space time. This holds as long as the ratio $T/k < 0.12$, i.e. in the region where the ratio of the threshold functions of the ultraviolet theory does not deviate strongly from unity (cf. figures 3,4). Thus temperatures smaller than roughly 140 MeV will not change the $T = 0$ couplings at finite temperatures at the ultraviolet scale $\Lambda = 1.2$ GeV.

Therefore we can use the same starting parameters as in the $T = 0$ theory to obtain finite temperature results and solve for each fixed temperature T the evolution equations as functions of k . The numerical results show the following behaviour:

With increasing temperature the mass parameter m_k decreases slightly more slowly towards the condensation point (cf. figure 5), but the main effect of the finite temperature occurs below $k \simeq 800$ MeV.

The threshold functions contain an additional damping due to the Matsubara frequency. Below the condensation point the boson condensate ϕ_k^2 reaches less high values at finite temperatures than at $T = 0$. It decreases with $k \rightarrow 0$ for all temperatures. This effect is due to the pion fluctuations. The critical temperature is reached when the condensate tends to zero. The exact value of the critical temperature depends on the interplay between the relevant sigma mass and quark mass in the intermediate k -region. If the “squared sigma mass” $2\lambda_k\phi_k^2$ is small relative to k^2 the sigma fluctuations drive symmetry restoration together with the pionic fluctuations. Our values of the relevant parameter $2\lambda_k\phi_k^2$ at $T = 0$ are typically around four times the quark constituent mass squared evaluated between $100 \text{ MeV} < k < 300 \text{ MeV}$. The sigma mass itself is well defined for all k in the case of explicit symmetry breaking. The particle data book [22] gives for the f_0 - or σ -meson a mass range between 400 MeV and 1200 MeV. From the nucleon nucleon interaction, however, we know that the intermediate range attraction comes from an equivalent sigma mass

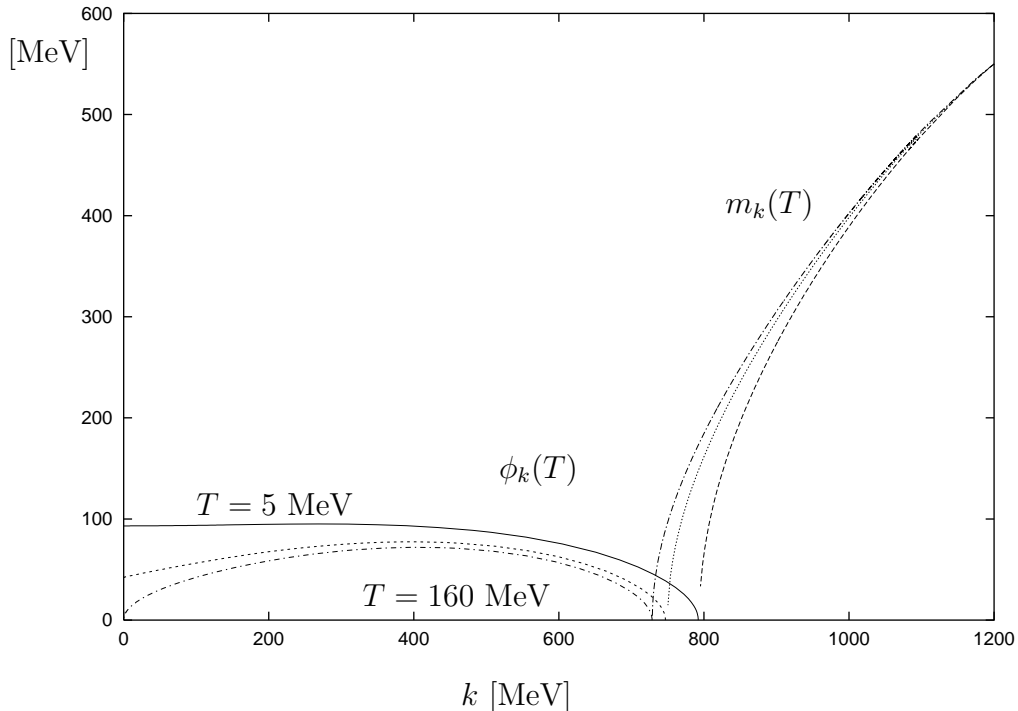


Figure 5: The VEV ϕ_k for $k < k_{\chi SB}(T)$ and the mass m_k for $k > k_{\chi SB}(T)$ for different temperatures. (Upper line $T = 5$ MeV, middle line $T = 150$ MeV and bottom line $T = 160$ MeV). The decrease of the order parameter ϕ_k towards zero for $k = 0$ signals the chiral phase transition.

which has a value of ≈ 560 MeV e.g. in the Reid soft core potential [23]. We add as a note of caution that even if the $O(4)$ dynamics determine critical indices at T_c correctly, the value of T_c may be influenced by gluonic degrees of freedom exterior to the linear σ -model in its present form. E. g. one can imagine that the σ couples to the glueball which dissolves at the critical temperature if the deconfinement transition occurs together with the chiral phase transition. With the linear sigma model as given and the above parameters we obtain a critical temperature:

$$T_c \approx 164 \text{ MeV} . \quad (42)$$

This temperature is higher than the critical temperature of the Wetterich group, even if $f_\pi = 93$ MeV had been used in [2] for the chiral limit. Wetterich et al. obtained a critical temperature $T_c \approx 100$ MeV. They also use different non-analytic threshold functions and wave function and coupling constant renormalization. But we do not expect the latter modifications to change the critical temperature drastically.

In figure 6 we show the order parameter $\phi_{k=0}(T)$ as a function of temperature. At a first glance one might think that the calculated behaviour follows roughly the chiral perturbation theory until $T \approx 110$ MeV, then it deviates because of strong massless mesonic fluctuations which are not properly taken into account in chiral perturbation theory. In detail our calculation coincides with chiral perturbation theory up to temperatures about 45 MeV then small deviations are visible. In chiral

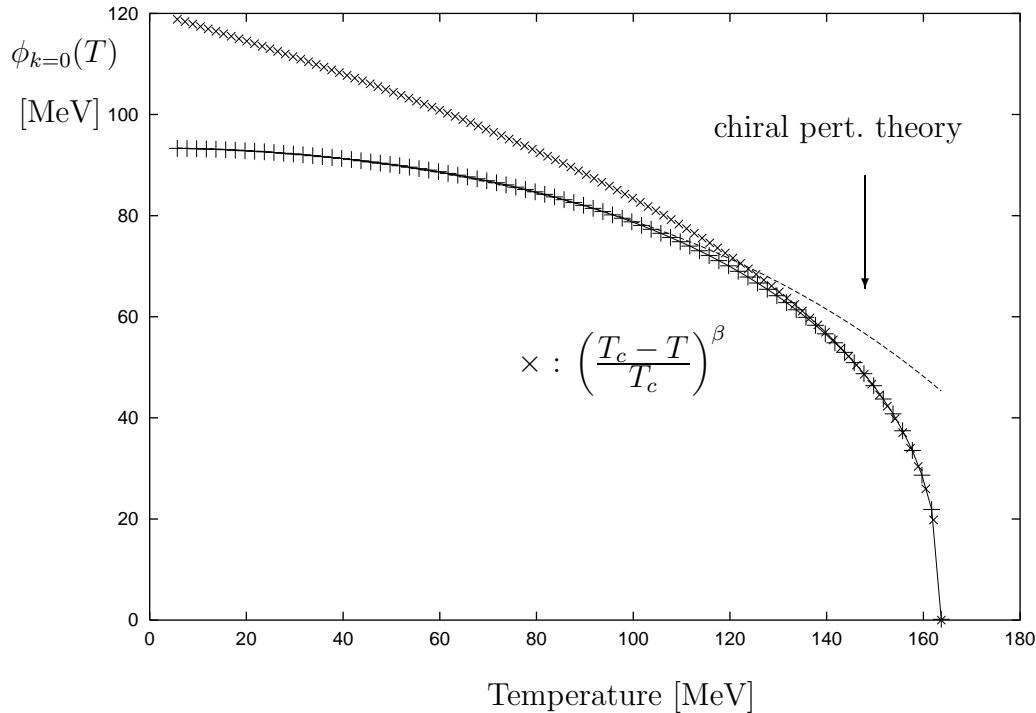


Figure 6: The order parameter $\phi_{k=0}$ as a function of the temperature T .

perturbation theory the temperature dependence of the light quark condensate for massless quarks, plotted in figure 6, is given by the expression

$$\frac{\langle \bar{q}q \rangle_T}{\langle \bar{q}q \rangle_0} = 1 - \frac{T^2}{8f_\pi^2} - \frac{T^4}{384f_\pi^4} - \frac{T^6}{288f_\pi^6} \ln \frac{\Lambda_q}{T} + \mathcal{O}(T^8) \quad (43)$$

with $\Lambda_q = 470 \pm 110$ MeV [14]. In a model without quark confinement like the one used here the fermion loop may be overestimated cf. [15]. In general the mesonic modes have Boltzmann suppression factors $\propto \exp(-2m_Q/T)$ compared to a Boltzmann factor $\propto \exp(-m_Q/T)$ for the quark degrees of freedom, where m_Q is the constituent quark mass. Therefore the mesons probably contribute to the pressure at somewhat higher temperatures than unconfined quarks.

The renormalization group calculation gives a non mean field behaviour for the order parameter at T_c , since the long range fluctuations of the softening σ modes are gradually taken into account by the successive lowering of the cutoff. The renormalization group flow equations at finite temperature sum the diverging thermal fluctuations properly near the critical point.

In the vicinity of T_c we obtain scaling behaviour of the order parameter with a critical exponent $\beta \approx 0.40$ as shown in figure 6. In fact it is possible to determine the exponent β by analyzing numerically the power law behaviour of the order parameter near T_c . We plot $\log(\phi_k)$ versus $\log((T_c - T)/T_c)$ in figure 7. The data points lie on a linear curve, thus ϕ_k scales like

$$\phi_k \propto \left| \frac{T - T_c}{T_c} \right|^\beta \quad (44)$$

with a critical exponent $\beta \approx 0.40$ which is in good agreement with lattice results for the $O(4)$ -theory in three dimensions [1]. We also compare the result with the mean field value $\beta = 0.5$ in figure 7.

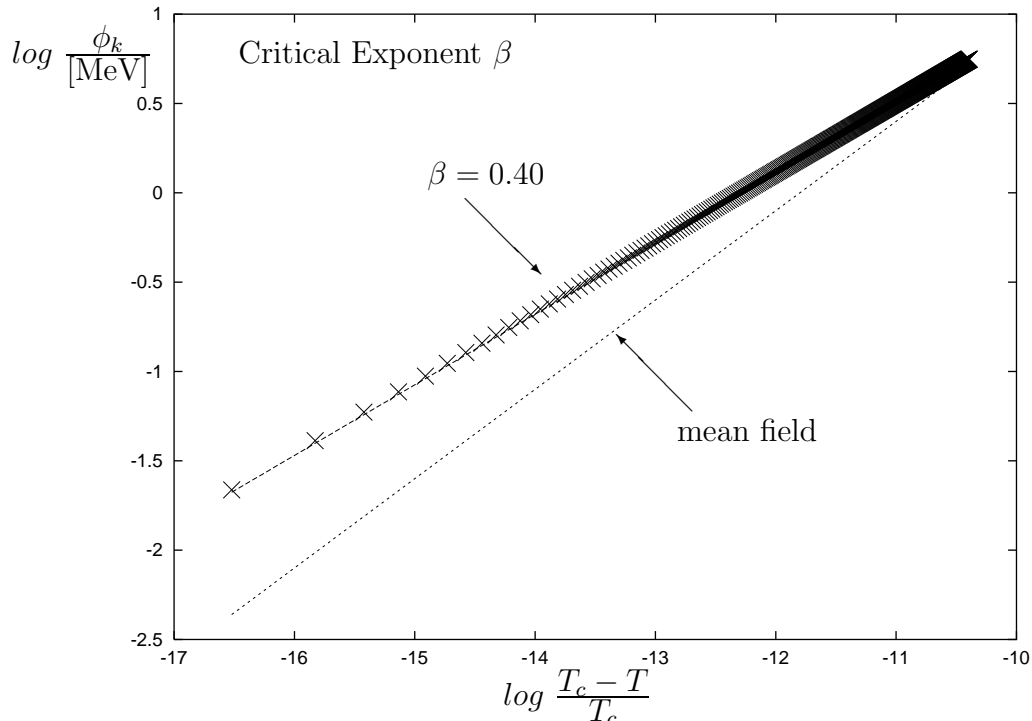


Figure 7: Determination of the critical exponent β from the temperature dependence of the order parameter ϕ_k .

At finite temperature the limit $T/k \rightarrow \infty$ enforces dimensional reduction. One knows, that the linear sigma model lies in the same universality class as the three-dimensional $O(4)$ -Heisenberg model, since the fermions are not contributing to the critical fluctuations near T_c [13]. Thus we deal with an effectively three-dimensional bosonic $O(4)$ -symmetric sigma model. For the $O(4)$ -theory there are six common critical exponents but only two of them are independent because they are related by four well-known scaling relations of the three-dimensional scalar $O(4)$ -model:

$$\begin{aligned} \alpha &= 2 - d\nu , \\ \beta &= \frac{\nu}{2}(d - 2 + \eta) , \\ \gamma &= (2 - \eta)\nu , \\ \delta &= \frac{d + 2 - \eta}{d - 2 + \eta} , \end{aligned}$$

where d is the dimension of the system ($d = 3$) [24]. Using these relations our results for $\beta = 0.40$ and $\eta = 0$ (no wave function renormalization is used) predict the values in tab. (1) which are denoted by RG.

Because we know the free energy density of the system we can calculate the specific heat directly, which is presented in the next section and verify the above predictions by a determination of the critical exponent α . We find numerically $\alpha = -0.39$ which is consistent with the scaling relation prediction and the $O(4)$

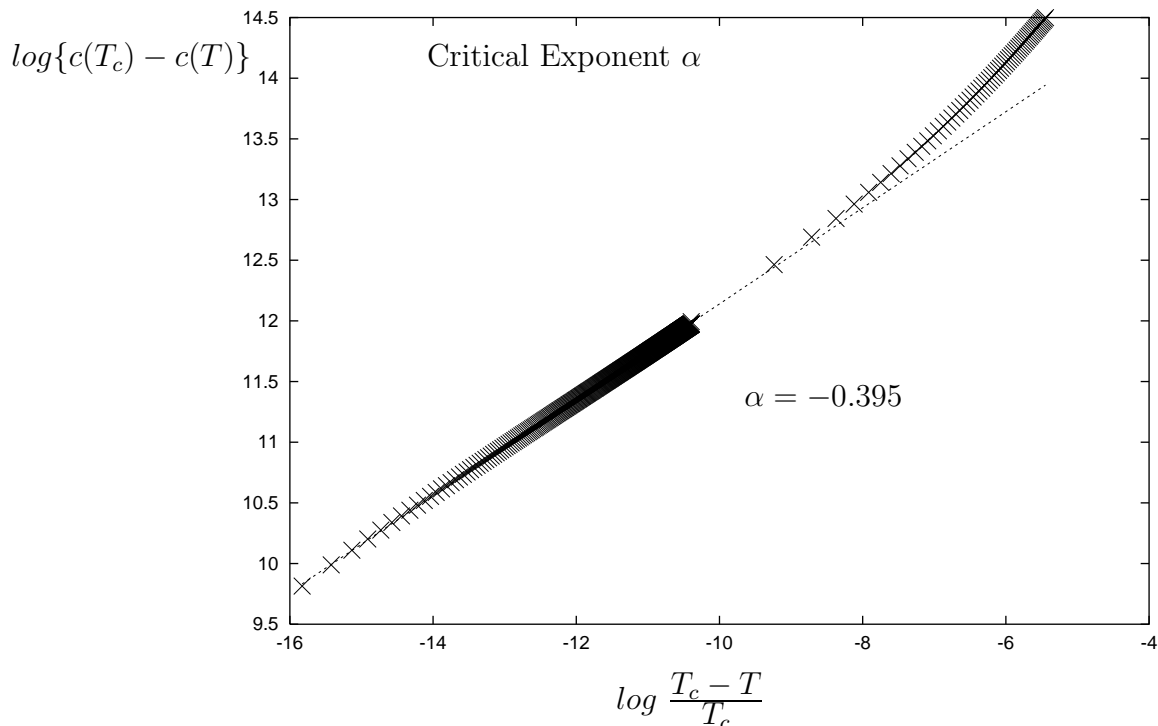


Figure 8: Determination of the critical exponent α for the specific heat $c(T) = c(T_c) + \text{const.}|T - T_c|^{-\alpha}$ in the vicinity of the critical temperature.

	Mean Field	RG	$O(4)$ Lattice	QCD Lattice
$1/\beta\delta$	$2/3$	0.5 ± 0.06	$0.537(7)$	$0.77(14)$
$1/\delta$	$1/3$	0.2	$0.2061(9)$	$0.21 \dots 0.26$
$1 - 1/\delta$	$2/3$	0.8	$0.7939(9)$	$0.79(4)$
$(1 - \beta)/\beta\delta$	$1/3$	0.3 ± 0.06	$0.331(7)$	$0.65(7)$
$\alpha/\beta\delta$	0	-0.2 ± 0.1	$-0.13(3)$	$-0.07 \dots +0.34$

Table 1: Critical exponents of the three dimensional $O(4)$ model in mean field, in our approach with numerical errors (RG) and lattice calculations compared to lattice QCD calculations with staggered quarks (QCD Lattice) (cf. ref. [1]).

scaling is confirmed (cf. fig. 8 and tab. (1)). One should note though, that the errors quoted for our results correspond to numerical errors but do not capture truncation errors.

An especially interesting point is to find the window for the critical dynamics. Further investigations away from the critical point may give an indication how far away from T_c the renormalization group improvement is important for the behaviour of the order parameter. In the superconducting phase transition only the mean field behaviour is experimentally relevant. Figure 6 shows that in chiral QCD the critical behaviour influences a wide range of temperatures, i.e. from $T = 130$ MeV to the critical temperature T_c . In real QCD, however, the finite quark masses spoil the

second order phase transition. Also gluon effects will change the behaviour of the pressure in comparison with the effective linear σ -model. Our findings for the critical exponents show excellent agreement with numerical simulation results of the lattice $O(4)$ -model.

Numerical simulations of lattice QCD, however, indicate a critical behaviour of the order parameters which is still ambiguous. The critical index δ gives a strong hint for dimensional reduction. For the exponent β a possible overlap exists. For the specific heat the QCD gluonic degrees of freedom may alter the behaviour significantly. The treatment of light quarks and pions with large correlation lengths is problematic on the lattice.

3.4 Free energy at finite temperature

Now we turn to the discussion of the equation of state for the linear σ -model in the chiral limit. We emphasize this point, because the physics of the model calculation is clarified by the equation of state. If the model is complete in the low virtuality region, the transmutation of quark-gluonic degrees of freedom occurs above the ultraviolet scale. Is this assumption justified?

Considerable care has been devoted to the treatment of critical fluctuations. In order to mark the progress achieved so far, the equation of state is the next goal. Of course one does not expect to see free gluons above T_c , but what kind of interaction effects among the quarks do we have? Can they be compared to deviations of the lattice results from the Stefan Boltzmann limit?

The most important thermodynamical tool for the analysis of a phase transition is the free energy, which is given as a logarithm of the partition function. The logarithm of the partition function is equal to the effective action, defined in eq. (15). Thus the solution of the flow equations, (35) and (38), yields the free energy density f as function of the temperature so that the pressure is given by

$$P(T) = -v_{k \rightarrow 0} = -f . \quad (45)$$

The internal energy density is defined by

$$u = \frac{d(\beta f)}{d\beta} \quad (46)$$

$$= -T^2 \frac{d(\beta f)}{dT} , \quad (47)$$

with $\beta = 1/T$ and the entropy density by

$$s = -\frac{df}{dT} . \quad (48)$$

These quantities are connected by the relation $P = Ts - u$.

Finally, the specific heat is given by a further temperature derivative of the free energy density

$$\begin{aligned} c_V &= -\beta^2 \frac{du}{d\beta} \\ &= \frac{du_k}{dT} . \end{aligned} \quad (49)$$

In order to find the temperature derivative of the free energy density one has to take into account the temperature dependence of the quartic coupling $\lambda_k(T)$ and the VEV $\phi_k(T)$. In principal the thermodynamic functions can be obtained by numerically differentiating the $k = 0$ value of the free energy density as a function of temperature. In practice the accuracy of this purely numerical differentiation is not sufficient, especially around the critical temperature. We therefore prefer to create for each phase a set of additional six evolution equations which contain the first and the second derivatives with respect to temperature of the original evolution equations, cf. eqs. (36),(37) for the symmetric phase and eqs. (39),(40) for the broken phase. Thus for each temperature derivative one has to solve three additional flow equations in this truncation schema, i. e. in total we have nine highly, non-linear coupled flow equations. Because they are lengthy and are given by a straightforward calculation we renounce to quote the result here.

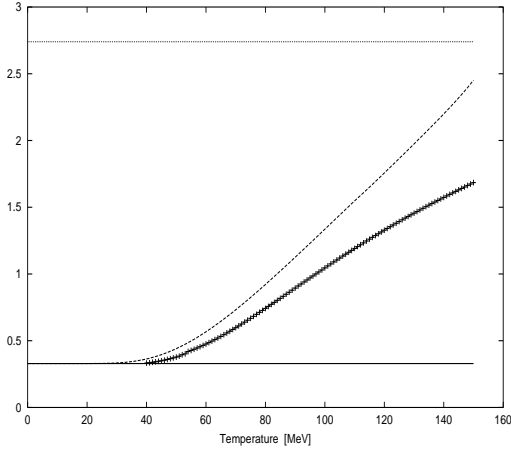


Figure 9: Pressure P/T^4

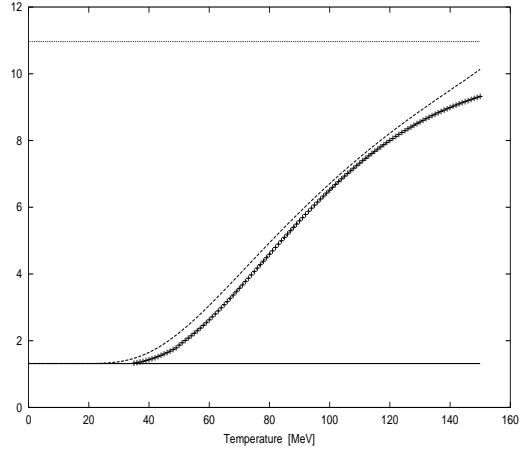


Figure 10: Entropy density s/T^3

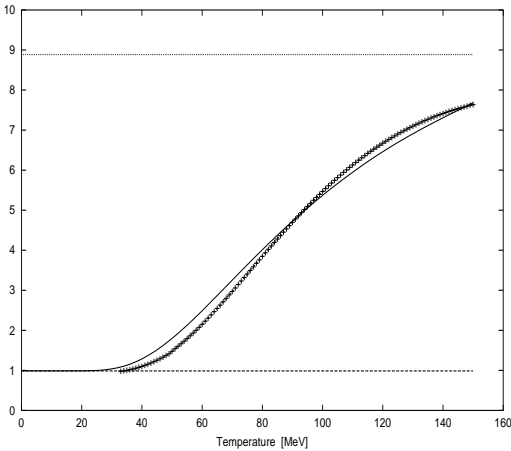


Figure 11: Internal energy density u/T^4

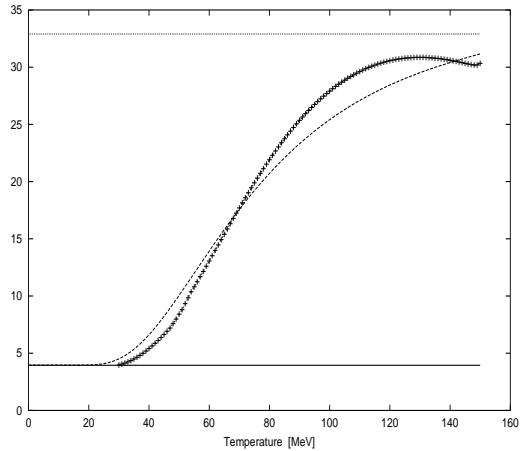


Figure 12: Specific heat c/T^3

The procedure to solve these equations is the same as before. The thermodynamic predictions are restricted to a temperature window, which is dictated by the omission of the temperature dependence of the initial values for the flow equations

at the ultraviolet cutoff scale (cf. discussion sec. 3.3). From this point of view a large scale to start the evolution is desirable in order to reach predictive power at least up to the critical temperature. For all calculated thermodynamic quantities we choose a ultraviolet cutoff $\Lambda = 1.52$ GeV, which is close to the Landau pole of the quartic coupling in the chiral limit. Due to this Landau pole inherent in the flow equations and the necessity to satisfy certain phenomenological conditions discussed below a higher choice for the ultraviolet scale is not possible. We also changed f_π to 88 MeV in the chiral limit, so that we obtain for the finite pion mass case the measured pion decay constant $f_\pi = 93$ MeV automatically (cf. sec. 4). With the new ultraviolet cutoff we need new initial values. We take $\lambda_\Lambda = 225$, which is larger than the one used before with a smaller cutoff due to the growth of the quartic coupling in the ultraviolet. We have to adjust the starting mass to $m_\Lambda = 1$ MeV, because for high cutoff with large λ_k the evolution equation of m_k^2 (cf. eq.(28)) is governed by the bosonic term proportional to λ_k which first drives the mass up for $\Delta k < 0$ before the fermion loop decreases m_k again.

For the flow equations we find for the critical temperature the smaller value

$$T_c = 149\text{MeV} , \quad (50)$$

which follows from the smaller f_π , but is still much higher than the value found by the Wetterich group [2].

The initial values for the additional flow equations at the ultraviolet scale Λ are zero. At the chiral symmetry breaking scale $k_{\chi SB} \approx 0.8$ GeV which is also a function of temperature the slopes of the flow equation for v_k in the symmetric phase (35) and in the broken phase (38) are identical. The evolution of the potential v_k with respect to k already stabilizes at small but finite k -values ($k \approx 150$ MeV).

The result for the normalized pressure (cf. eq. (45)), scaled with the temperature P/T^4 , is plotted in figure 9 and in figure 10 the scaled entropy density s/T^3 (crosses) is shown. In figure 11 the scaled internal energy density u/T^4 and in figure 12 the scaled specific heat c/T^3 are shown for the chiral limit.

In order to compare our results with a gas of non-interacting quarks, antiquarks and pions, we evaluate the corresponding thermodynamic functions with the temperature dependent masses evolved to $k \approx 0$ (dashed lines in the figures).

For small temperature the quarks are massive and therefore thermodynamically suppressed by their Boltzmann factor. The main contribution to all presented thermodynamic observables in that temperature limit stems from the massless pions.

We stop the flow equation at a small infinitesimally finite scale k and obtain a finite sigma meson mass due to a finite quartic coupling. We have checked that there is no influence of a sigma degree of freedom to the thermodynamic functions at finite temperature, because the relevant quantity for decoupling is the mass squared over k^2 .

Due to the linear evolution of the quartic coupling with k for $k \ll T$ which tends to zero for $k = 0$ in the chiral limit, the sigma meson decouples from the low momentum mode thermodynamics and we obtain the expected Stefan-Boltzmann limit of a massless pion gas for small temperatures.

The respective thermodynamic functions for three pionic degrees of freedom are

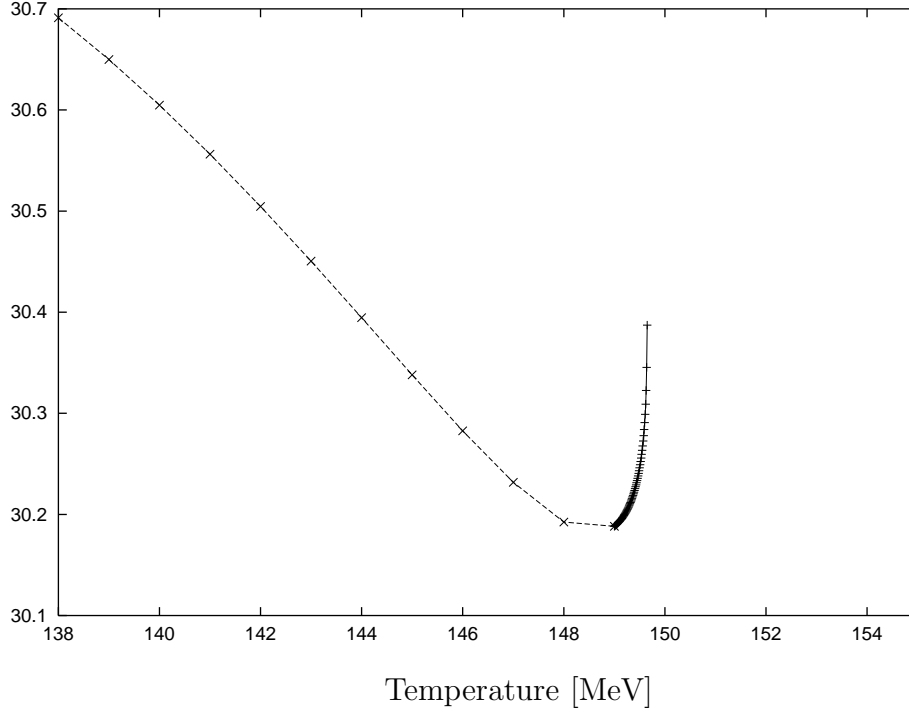


Figure 13: Specific heat c/T^3 in the vicinity of the critical temperature.

given by

$$P/T^4 = 3\frac{\pi^2}{90} \approx 0.33 \quad (51)$$

$$u/T^4 = 3P/T^4 = 3\frac{\pi^2}{30} \approx 0.99 \quad (52)$$

$$s/T^3 = 4P/T^4 = 12\frac{\pi^2}{90} \approx 1.32 \quad (53)$$

$$c/T^3 = 4\frac{\pi^2}{10} \approx 3.95 \quad (54)$$

In each figure 9-12 the lower horizontal lines represent the pion gas limit. With increasing temperature all observables except the pressure follow roughly the ideal gas behaviour. At the critical temperature the quarks are massless and the Stefan-Boltzmann limit for a massless quark-antiquark and massless pion-sigma meson gas is depicted by the upper horizontal line in the figures. The thermodynamic functions for a gas with $N_c N_f$ massless quarks can be calculated analytically:

$$P/T^4 = N_c N_f \frac{28\pi^2}{720} \approx 2.30 \quad (55)$$

$$u/T^4 = 3P/T^4 = N_c N_f \frac{28\pi^2}{240} \approx 6.9 \quad (56)$$

$$s/T^3 = 4P/T^4 = N_c N_f \frac{112\pi^2}{720} \approx 9.21 \quad (57)$$

$$c/T^3 = N_c N_f \frac{28\pi^2}{60} \approx 27.63 \quad (58)$$

For the numerical calculations at finite temperature one can not simplify the computer effort. In ref. [2] the authors reduced the complicated and time intensive calculations by substituting the simpler zero temperature flow equations for the finite temperature flow equations as long as $k \geq 10T$. For smaller scales they used the finite temperature flow equations. This is certainly a good approximation for the quantities considered there. But the low temperature equation of state would not be described correctly in such an approximation. We therefore use during the whole evolution the finite temperature flow equations and optimize the convergence of the Matsubara series by an generalized Θ -function transformation, which is described in the appendix. In practice we take more than $N = 4000$ Matsubara frequencies into account in the low temperature region ($k \gg T$) in order to adequately solve the equations over the hole scale range. For higher temperatures ($k \ll T$) only a few Matsubara modes are important.

On the other hand our ultraviolet scale might be identified with the scale [2], where the meson bound states appear. Due to the neglect of the wave function renormalization we do not suppress the kinetic terms of the mesons at the compositeness scale. This has an important consequence: Fixing the Yukawa coupling g at the compositeness scale to its infrared value which yields a finite constituent quark mass of roughly $m_q \approx 300$ MeV, we do not encounter the partial approximate infrared fixed point, found in [2], which would weaken the dependence of the infrared physics on the chosen initial values. In our case we can choose a high ultraviolet scale and are nevertheless able to adjust the infrared quantities like e. g. the pion decay constant.

To improve the finite temperature results we use a so-called generalized Θ -function transformation which accelerates the convergence of the Matsubara sums leading to modified Bessel function $K_\nu(x)$. This reformulation has the pleasant side effect to separate analytically the thermal fluctuations from the $T = 0$ fluctuations. The right hand sides of the flow equations split into the pure zero temperature flow equation part and a finite temperature part. We are aware that the separation of these terms does not decouple the quantum from the thermal fluctuations because of the nonlinearity of the evolution.

This property, however, allows a clean normalization: neglecting the finite temperature part of the corresponding flow equation yields the correct zero temperature contribution.

In our approximation of neglecting the scale and temperature dependence of the Yukawa coupling as well as the quark and meson wave function renormalization, the constituent mass follows the temperature behaviour of the order parameter $\phi_k(T)$. In the chiral limit above the critical temperature of $T_c \approx 150$ MeV the quark masses are identically zero and the mesonic masses are degenerate and increase with temperature because the mesonic coupling also increases with temperature in the symmetric phase. For finite pion masses this behaviour is smoother, but qualitatively similar and will be discussed in the next section.

4 Equation of state for finite pion mass

It is straightforward to derive thermodynamic quantities for finite pion masses by introducing an explicit symmetry breaking term c in the potential. The explicit symmetry breaking constant c is kept fixed and is proportional to the current quark mass.

We find the following mass identifications:

$$\text{pions: } m_{\pi,k}^2(T) = c/\phi_k(T) \quad (59)$$

$$\text{sigma: } m_{\sigma,k}^2(T) = c/\phi_k(T) + 2\lambda_k(T)\phi_k^2(T) \quad (60)$$

$$\text{quarks: } M_{q,k}(T) = g\phi_k(T) \quad (61)$$

It is not clear if the σ -mass, given above, is actually the physical σ -mass and necessarily a pole in the two-point Greens function. We follow ref. [2] where this expression is also denoted as the σ -mass and corresponds to the radial mode of the $O(4)$ model.

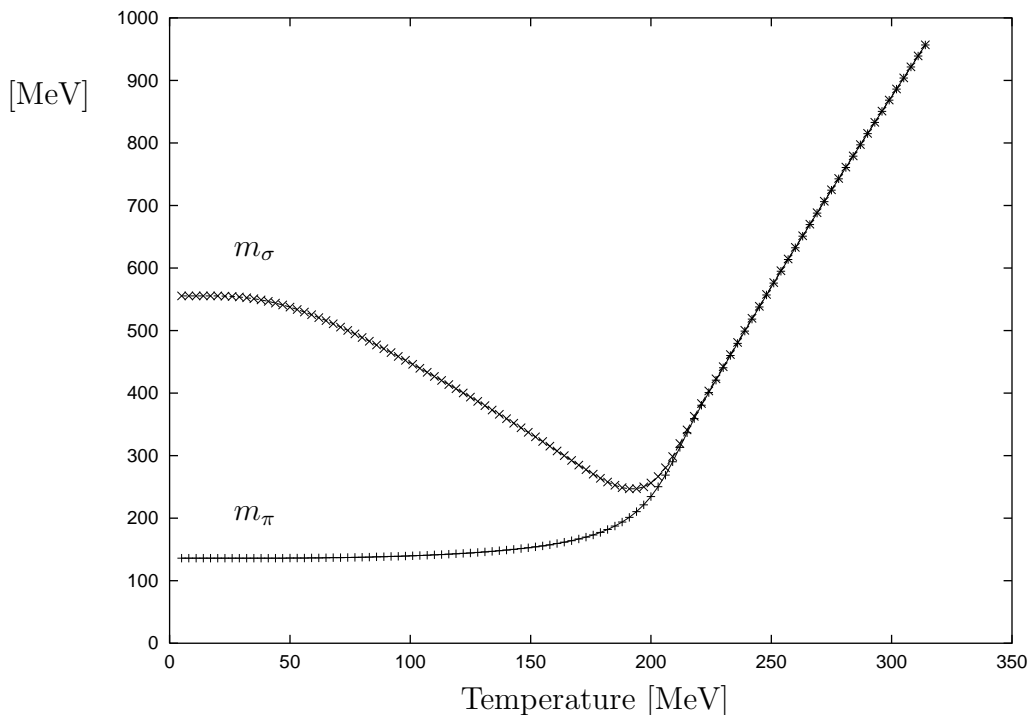


Figure 14: Mesonic masses versus temperature.

We fix the constant c via the pion mass ($m_\pi(T=0) = 135$ MeV) to $c = 1.7 \cdot 10^6$ MeV³, which results in a sigma-mass of about 550 MeV at vanishing temperature. In reference [2] the sigma mass is considerably smaller. For finite pion masses the two sets of flow equations for each phase in the chiral limit merge together to one set of flow equations. The constituent quark mass follows the order parameter and never becomes zero in the symmetric phase for high temperature due to a smooth crossover between both phases. The evolution equations for finite pion masses have been studied for two different cutoffs $\Lambda = 1.2$ GeV and $\Lambda = 2.0$ GeV. Due to the symmetry breaking term in the potential the initial values are not so sensitive to a change of cutoff. The respective initial values are for $\Lambda = 1.2$ GeV $\lambda = 115$, $m = 1$

MeV and $\lambda = 430$, $m = 1$ MeV for $\Lambda = 2$ GeV. In fig. 14 the resulting mesonic masses are shown as function of temperature. The scalar meson mass drops relatively quickly with temperature while the pseudoscalar masses are almost temperature independent in the broken phase. We think that a wave function renormalization correction for the scalar fields does not change this situation dramatically at least in the broken phase.

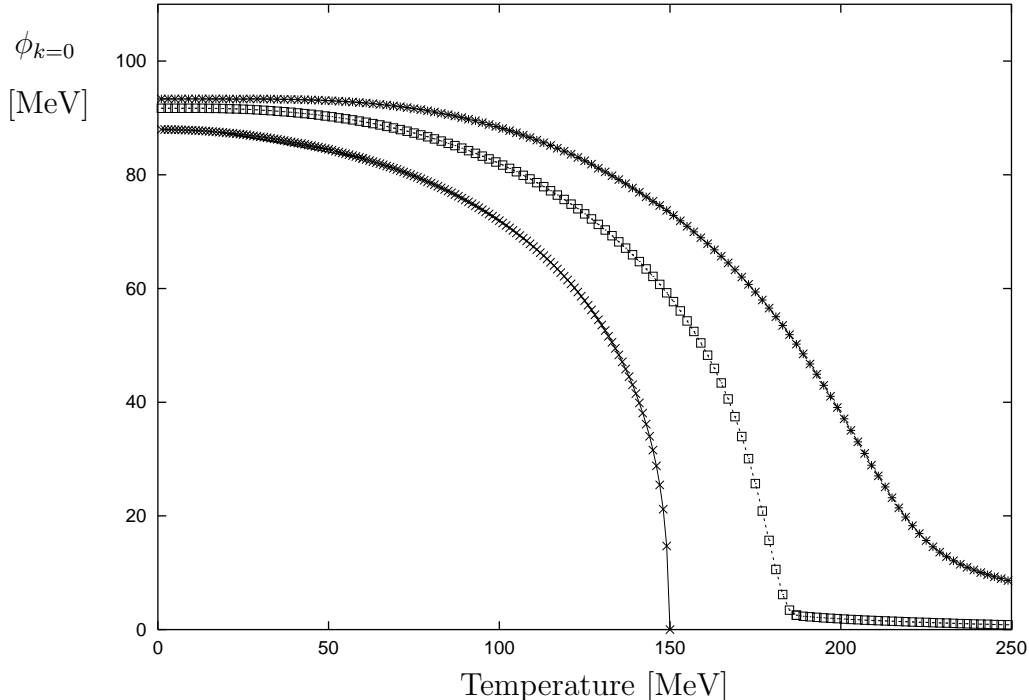


Figure 15: The order parameter $\phi_{k=0}$ for different pion masses. (Lower curve: chiral limit; middle curve: $m_\pi \approx 45$ MeV; upper curve: $m_\pi \approx 135$ MeV).

In general the derivative of these masses with respect to temperature is independent of the choice of the initial UV cutoff. The increase of the masses with temperature in the restored phase, however, depends slightly on the choice of the UV starting cutoff. We consider this as an artefact of the omission of wave function renormalization, which would influence the temperature increase of the quartic coupling in the restored phase.

In fig. 15 we compare the order parameter for different pion masses. The lower curve represents the chiral limit where one sees a second order phase transition. This transition is smeared out if one switches to finite pion masses. The middle curve is achieved for a pion mass of roughly 45 MeV and the upper curve shows the realistic case. Note that the order parameter at zero temperature increases with the pion mass automatically. If one defines a pseudocritical temperature analog to ref. [2] as the inflection point of the order parameter one observes an increase of the critical temperature with the pion mass from $T_c \approx 150$ MeV for the chiral limit up to $T'_c \approx 190$ MeV for a pion mass $m_\pi = 135$ MeV. Due to the finite symmetry breaking term in the potential the order parameter never vanishes at high temperature.

Above the critical temperature of the chiral transition about 200 MeV we see a parity doubling of the scalar and pseudoscalar particles, which is a signal of chiral

restoration and the masses for the mesons rise proportional to temperature due to the increase of the effective mass term with temperature and the symmetry breaking term. This behaviour is similar to the behaviour of meson correlation functions for massless free quarks above T_c on the lattice [26].

The hadronic screening masses at high temperature are controlled by the lowest Matsubara frequency of quarks and increase therefore like $2\pi T$. The physics in our case is probably more related to the meson dynamics.

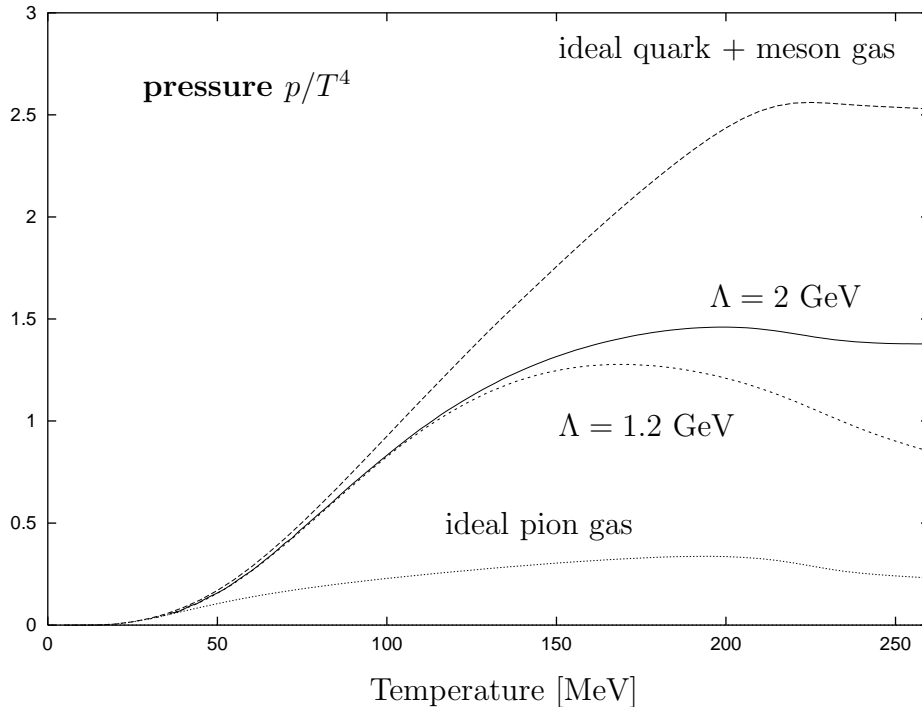


Figure 16: Scaled pressure $(P(T) - P(T = 0))/T^4$ for different systems as function of temperature (see text for details).

In the remaining section we focus on the thermodynamic. In general the following physical scenario becomes evident: For low temperature the quarks and mesons are massive, while in the partition function with unbroken chiral symmetry the pions remain massless³. In the chiral limit for low temperature one expects and indeed obtains that the physical observables are dominated by a massless non-interacting pion gas and that the Stefan-Boltzmann limit is saturated. On the other hand, for high temperature in the thermally restored chirally symmetric phase the quarks are exactly massless while both, the pions and the sigma mesons, have finite (degenerated) masses due to the restoration of chiral $SU(2) \times SU(2)$ symmetry. Thus all thermodynamic quantities at high temperature are dominated by the massless quarks with $N = 4N_c N_f$ degrees of freedom modified by their interaction.

A similar but not identical situation holds for finite quark masses. The low temperature gas is hadronic made out of pions mostly, the high temperature plasma is a quark plasma. At the critical point the sigma mass is small. Therefore, except

³ In this case the so-called sigma meson mass, which is proportional to the quartic coupling tends to zero in the IR region.

near the critical temperature the physical sigma meson contribution to the thermodynamic functions for low and high temperature can nearly be neglected. In the following figures we show the pressure P/T^4 (cf. fig. 16) and the scaled internal energy density u/T^4 (fig. 17) and the scaled entropy density s/T^3 (fig. 18). In all figures we compare the results with a non-interacting quark-meson gas (uppermost curve) and also with a ideal pion gas (lowest curve).

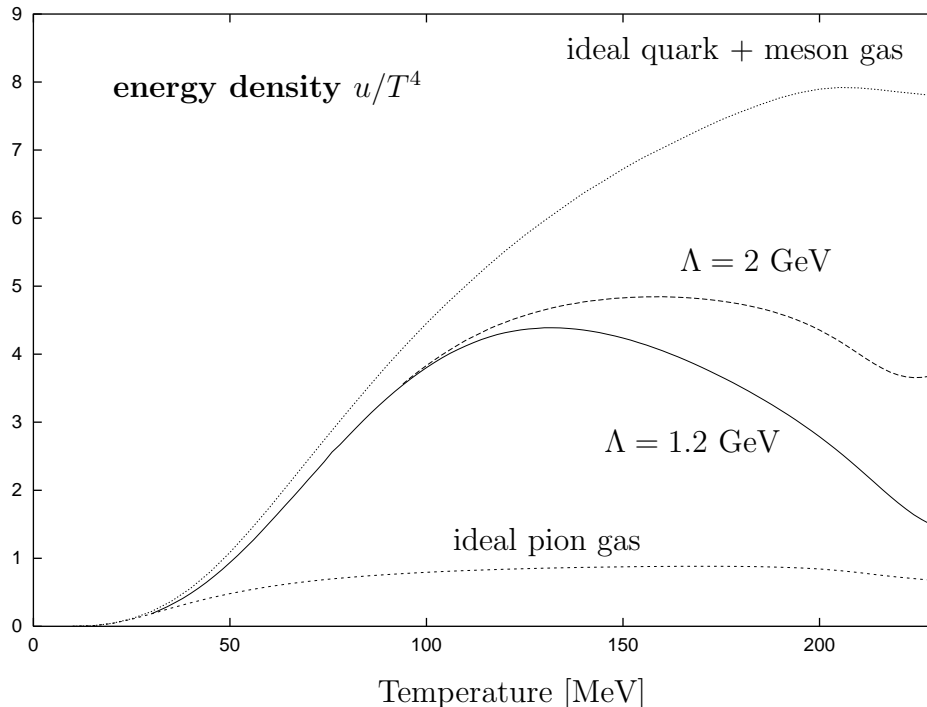


Figure 17: Scaled energy density u/T^4 for different systems as function of temperature (see text for details).

For finite masses the pressure for small temperature is exponentially suppressed as expected. At $T \approx 200$ MeV the total pressure caused by interacting pions, sigma and constituent quarks reaches the maximum at $(P(T) - P(T = 0))/T^4 = 1.46$, decreases in the following a bit and settles down around $T \approx 300$ MeV at 1.37 (see fig. 16).

A pressure due to the quarks exists also for small temperature, which is a consequence of the fact that the quarks are not confined in the model. For zero temperature there is no pressure because the quarks are massive but with increasing temperature, the pressure rises and at temperatures around $T \approx 70$ MeV the quark pressure is comparable with the mesonic pressure. In fig. 16 the lowermost curve shows the pressure of $N = 3$ pions.

With increasing temperature the quark contribution takes over and the total pressure saturates at $\sim 55\%$ of the Stefan-Boltzmann limit for $T > 250$ MeV. This result is comparable with an NJL model calculation for small temperature using a RPA approximation including fluctuations. Even below the critical temperature a strong cutoff dependence enters into the results of previous calculations [29].

At very high temperatures $T > 180$ MeV our model is no longer adequate: the pressure depends on the ultraviolet cutoff which suppresses high momenta. There-

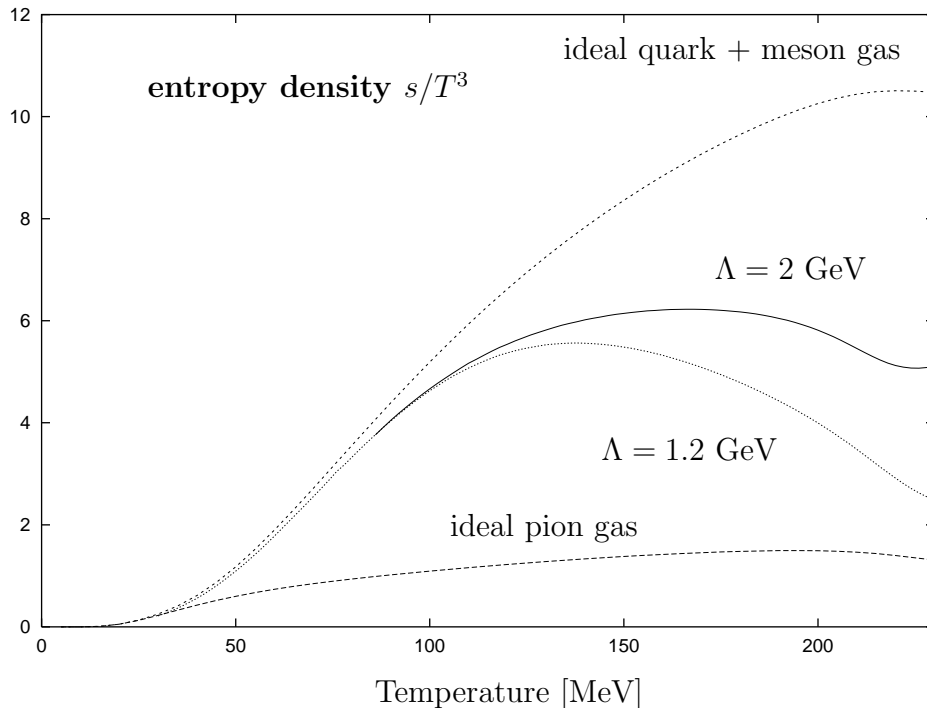


Figure 18: Scaled entropy density s/T^3 versus temperature for different systems (see text for details).

fore all non-universal thermodynamical quantities have a tendency to be too small at too high temperatures. In order to demonstrate this property we have plotted two curves in the figures. The lower line displays the pressure for an ultraviolet cutoff $\Lambda = 1.2$ GeV while the upper curve is calculated with $\Lambda = 2.0$ GeV. One sees nicely which temperatures can be described for a given cutoff. Both curves coincide up to a temperature of $T \approx 120$ MeV, the lower curve turns off for higher temperature. Indeed it should be valid only up to $T \approx 120$ MeV. We have checked that the results in the shown temperature region are stable with respect to a further increase of the ultraviolet cutoff beyond $\Lambda = 2.0$ GeV.

The uppermost curve in figure 16 displays the total contribution of a non-interacting gas of quarks and mesons calculated with temperature dependent masses, which are extracted out of the flow equations. It reaches almost the Stefan-Boltzmann limit ($P/T^4 = 2.7$) around $T \approx 230$ MeV due to the decrease of the vacuum expectation value and therewith decreasing quark masses. On the other hand, the pions and sigma-meson pressure increases (m_σ decreases) up to $T \approx 200$ MeV and settles down in the symmetric phase on a constant value. This reflects the fact, that the meson masses increase proportional to the temperature and the ratio mass over temperature is almost constant. The pressure from the flow equation is considerably smaller than this limiting Stefan Boltzmann Plasma.

In fig. 17 the energy density, scaled by T^4 , is shown as function of the temperature. The interpretation of the results and notation of this figure is analogous to the pressure calculation. In the chiral limit at low temperatures we observe again the Stefan-Boltzmann limit $u/T^4 = \pi^2/10$ of the massless pion modes ($N = 3$). For finite pion mass at high temperatures the dependence on the ultraviolet cutoff is

slightly stronger compared to the pressure calculation.

The entropy density, scaled by T^3 , is plotted as function of temperature in fig. 18 and is obtained as a derivative with respect to the temperature of the free energy density, $s = -\partial f/\partial T$. The low and high temperature features of this quantity can be understood in a similar fashion as the pressure and energy density. For finite pion masses the entropy density is continuous in the vicinity of the chiral critical temperature ($T_c \approx 150$ MeV) and reaches 60% of the Stefan-Boltzmann limit around these temperatures, which equals to $s/T^3 = 8N_c \cdot 31\pi^2/720 + 16\pi^2/90 = 11.95$. Due to finite meson masses which increase proportionally to temperature in the symmetric regime, the bosonic contribution to all thermodynamic quantities is strong suppressed. All shown thermodynamic quantities are reliable in a temperature window of $0 \leq T \leq 180$ MeV for an ultraviolet cutoff Λ of 2.0 GeV.

5 Conclusions

We have presented a new method to solve field theoretic problems at finite temperature. It is based on a nonperturbative application of the renormalization group. By successively integrating out modes in Euclidean momentum shells we can handle the nonlinear field couplings in a nonperturbative way, especially when long wavelength modes generate singular infrared behaviour near the critical temperature.

We apply a cutoff function in Schwinger proper time which combines a virtuality- or mass- like exponential cutoff with a polynomial which makes the calculation of the derivative of the effective potential with respect to the evolution scale insensitive to the ultraviolet modes. This reflects the modern view of renormalization theory, all field theories are effective theories with an ultraviolet cutoff and we always follow their infrared behaviour. The evolution equations are finite and well behaved, which a simple mass type cutoff would not guarantee. The specifically chosen heat kernel cutoff function has the additional advantage that all resulting evolution equations can be expressed in a very transparent and analytic form. In the one loop approximation propagator like functions for the individual particles appear with denominators which contain the respective masses depending on the effective potential. The renormalization group allows to improve the one loop approximation to sum in an optimal way the infrared singular fluctuations due to massless boson modes.

In this paper we have in addition truncated the effective potential to its lowest terms in the boson fields compatible with chiral symmetry. This is a simplification which is not necessary and can be improved [16],[17]. Also the consideration of coupling constant and more importantly wave function renormalization evolution equations is planned. The inclusion of vector and axial-vector mesons at finite temperature to study their mixing is also possible within this method and work in this direction is in progress [19].

This new method has been applied to the finite temperature phase transition from a constituent quark gas interacting with mesons to a massless quark phase in the framework of the linear sigma model. The underlying assumption of a reduction of the QCD degrees of freedom to an effective hybrid quark meson field theory at an ultraviolet scale of about 1 GeV has been analyzed via the resulting equation

of state. Of course, qualitatively the pressure is always dominated by the massless modes which are the pions at low temperature and the quarks at high temperature. But our calculation has highlighted finer features of the finite temperature behaviour.

The evolution equations decouple the quarks from further evolution when T/k becomes too large. This does not mean, however, that the quarks do not contribute to the pressure below the chiral phase transition. The renormalization group technique cannot mimic confinement when the field theoretic model does not contain this dynamical aspect. The equation of state at high temperatures shows considerable deviations from a free system of massless quarks. In our interpretation of the chiral phase transition long wavelength fermion modes really have zero masses at T_c . Quarks with moderate or higher virtualities are still massive and only at temperatures considerably higher than T_c the whole virtuality spectrum of modes is massless.

The real strength of the renormalization group lies near the critical temperature where the σ modes become massless. Here the linear sigma model with quarks is entirely dominated by the bosonic sector. The evolution equations reproduce well the universal critical behaviour of the model. We have calculated the critical indices β and α which are in good agreement with lattice simulations of the $O(4)$ theory. The missing wavefunction renormalization correction is known to be small. The evolution equations at finite temperature contain the physics of dimensional reduction: For $T/k > 0.3$ the bosonic loop contributions reduce to their zero Matsubara frequency part, i.e. they become equivalent three dimensional loops with effective couplings which have acquired temperature factors. The fermions decouple in this region of T/k . The differences of some of the critical indices to the mean field behaviour are small, i.e. $\beta = 0.4$ compared to $\beta_{mf} = 0.5$. This does not mean, however, that the region around T_c where the critical dynamics is important is small in the equation of state.

The phenomenological relevance of the critical behaviour is more limited because of the finite quark mass which breaks chiral symmetry explicitly and smoothes out all remarkable features of the $O(4)$ behaviour. In that respect the chiral dynamics is mostly important as a theoretical benchmark. It remains to be seen how far the critical $O(4)$ behaviour is seen in full QCD simulations.

The evolution equations have the unique property to unify different aspects of the hadronic system which conceptually and experimentally are widely separated. The zero temperature evolution gives a view of the field theoretic system with different resolution. The virtuality cutoff k is intimately related to the resolution of a probe with which we may study the system e.g. with photons in deep inelastic scattering. At high resolution we see a massless partonic system, at low resolution we encounter massive constituent quarks. There are not separate hadronic theories for different length scales: a high energy, an intermediate energy and a low energy theory, ideally they all evolve smoothly into each other. The challenge of hadronic physics lies in the fact that the important degrees of freedom transmute in a strongly coupled theory, very much different from a weakly interacting theory. Studying the hadronic system at finite temperature and/or finite density allows to emphasize different modes by varying the external parameter and thereby showing the transition of the dynamics explicitly. The evolution equations unify these different aspects of QCD which when studied separately look like rather independent developments in

hadronic and nuclear physics.

Acknowledgments

We would like to thank C. Wetterich, D.-U. Jungnickel and J. Berges for their introduction to the subject. B.J.S. expresses his gratitude to J. Wambach and D.-U. Jungnickel for numerous enlightening discussions on large parts of this work. He also would like to thank O. Bohr and Z. Aouissat for long and valuable discussions. H.J.P. especially would like to acknowledge discussions with N. Tetradis who has triggered this work.

A Matsubara Series:

In this appendix we summarize the low temperature limit of all in this work used Matsubara summations. They can be found by a comparison of the finite temperature flow equations with the zero temperature equations. The expression of eq. (41) can be generalized by

$$x \sum_{n=-\infty}^{\infty} \frac{1}{(1 + \tilde{\omega}_n^2 + \tilde{y}^2)^\alpha} \quad x \xrightarrow{0} \frac{2 \cdot 4 \dots (2\alpha - 3)}{1 \cdot 3 \cdot 5 \dots (2\alpha - 2)} \frac{1}{\pi} \frac{1}{(1 + \tilde{y}^2)^{(2\alpha-1)/2}} \quad (62)$$

with $x := T/k$, $\tilde{\omega}_n^2 := \omega_n^2/k^2$ and $\tilde{y}^2 := y^2/k^2$ and $\alpha = \frac{3}{2}, \frac{5}{2} \dots$ being a fractional power. We set $(2\alpha - 3) =: 1$ for $\alpha = \frac{3}{2}$.

For the derivatives with respect to temperature of the respective Matsubara sums we find for the low temperature limit ($l = 1$ describes the first derivative and $l = 2$ the second one)

$$x^{2l+1} \sum_{n=-\infty}^{\infty} \frac{(2n)^{2l}}{(1 + \tilde{\omega}_n^2 + \tilde{y}^2)^\alpha} \quad x \xrightarrow{0} \frac{2l - 1}{(2\pi^2)^l (\alpha - 1)(\alpha - 2) \dots (\alpha - l)} \frac{2 \cdot 4 \dots (2\alpha - 3 - 2l)}{1 \cdot 3 \cdot 5 \dots (2\alpha - 2 - 2l)} \frac{1}{\pi} \frac{1}{(1 + \tilde{y}^2)^{(2\alpha-1-2l)/2}} \cdot \quad (63)$$

If one replaces $n \rightarrow n + \frac{1}{2}$ in the last equation one gets the corresponding fermionic Matsubara sums with the same low temperature limit. In the low temperature limit the difference between the fermionic and bosonic Matsubara sums vanishes.

B Generalized Θ -function transformation:

In order to accelerate the convergence of the Matsubara sums appearing in the flow equations it is useful to apply a generalized Θ -function transformation. This transformation is based on the following equations:

For bosonic Matsubara modes and positive integer p we obtain⁴

$$\sum_{n=-\infty}^{\infty} (\gamma n^2)^p e^{-\gamma n^2} = \sqrt{\frac{\pi}{\gamma}} \frac{(2p-1)!!}{2^p} \left[1 + 2 \sum_{n=1}^{\infty} e^{-\pi^2 n^2 / \gamma} \sum_{l=0}^p \left(\frac{-\pi^2 n^2}{\gamma} \right)^l C_p^l \right] \quad (64)$$

⁴ A proof can be found in [30].

with $(2p - 1)!! = 1 \cdot 3 \dots \cdot (2p - 1)$ and

$$C_p^l = \frac{2^{2l} p!}{(2l)!(p-l)!},$$

and for the fermionic case [31]

$$\sum_{n=-\infty}^{\infty} (\gamma(n+1/2)^2)^p e^{-\gamma(n+1/2)^2} = \sqrt{\frac{\pi}{\gamma}} \frac{(2p-1)!!}{2^p} \left[1 + 2 \sum_{n=1}^{\infty} (-1)^n e^{-\pi^2 n^2 / \gamma} \sum_{l=0}^p \left(\frac{-\pi^2 n^2}{\gamma} \right)^l C_p^l \right] \quad (65)$$

This transformation can be applied to the finite temperature expression of the effective potential eq. (16) and the proper time integration can be performed analytically resulting in modified Bessel functions $K_\nu(x)$.

With the following convenient abbreviations (B = bosons and F = fermions)

$$\begin{aligned} h_\pi &:= \frac{1}{1 + c/(k^2 \phi_k)} \\ h_\sigma &:= \frac{1}{1 + (c/\phi_k + 2\lambda_k \phi_k^2)/k^2} \\ h_q &:= \frac{1}{1 + g^2 \phi_k^2 / k^2} \end{aligned} \quad (66)$$

and

$$\begin{aligned} B_\nu(x_m) &:= h_m^{\nu/2} \sum_{n=1}^{\infty} n^\nu K_\nu(nx_m) \quad m = \sigma, \pi \\ F_\nu(x_q) &:= h_q^{\nu/2} \sum_{n=1}^{\infty} (-1)^n n^\nu K_\nu(nx_q) \quad \nu : \text{integer} \end{aligned}$$

$$x_\pi := \frac{k}{T} h_\pi^{-1/2} \quad x_\sigma := \frac{k}{T} h_\sigma^{-1/2} \quad x_q := \frac{k}{T} h_q^{-1/2}$$

we obtain the flow equation e.g. for the free energy density:

$$k \frac{\partial v_k(T)}{\partial k} = \frac{k^4}{2(4\pi)^2} \left[3h_\pi + h_\sigma - 8N_c h_q + \frac{2k}{T} [3B_1(x_\pi) + B_1(x_\sigma) - 8N_c F_1(x_q)] \right] \quad (67)$$

Here one sees the separation of quantum and thermal fluctuations: The right hand side of the flow equation splits into the zero temperature flow equation part and a finite temperature part.

References

- [1] K. Kanaya and S. Kaya, Phys. Rev. **D51** (1995) 2404; K. Kanaya, Nucl. Phys. Proc. Suppl. **B47** (1996) 144.
- [2] D.-U. Jungnickel and C. Wetterich, Phys. Rev. **D53** (1996) 5142; J. Berges, D.-U. Jungnickel and C. Wetterich, Phys. Rev. **D59** (1999) 034010.
- [3] K. G. Wilson, Phys. Rev. **B4** (1971) 3174; K. G. Wilson and I. G. Kogut, Phys. Rep. **12** (1974) 75 ; J. Polchinski, Nucl. Phys. **B231** (1984) 269.
- [4] F. Wegner and A. Houghten, Phys. Rev. **A8** (1973) 401; F. Wegner in *Phase Transitions and Critical Phenomena*, vol. 6, eds. C. Domb and M.S. Greene, Academic Press (1976).
- [5] R. D. Ball, Phys. Rev. **182** (1989) 1.
- [6] U. Ellwanger and C. Wetterich, Nucl. Phys. **B423** (1994) 137.
- [7] J. I. Kapusta, *Finite Temperature Field Theory* (Cambridge University Press, 1989); M. Le Bellac, *Quantum and Statistical Field Theory* (Oxford Science Publications, 1991).
- [8] T.R. Morris and M.D. Turner, Nucl. Phys. **B509** (1998) 637.
- [9] A. Hasenfratz and P. Hasenfratz, Nucl. Phys. **B270** (1986) 685; P. Hasenfratz and J. Nager, Z. Phys. **C48** (1988) 477.
- [10] L. Dolan and R. Jackiw, Phys. Rev. **D9** (1974) 3320.
- [11] H. G. Dosch, T. Gousset and H. J. Pirner, Phys. Rev. **D57** (1998) 1666.
- [12] B.-J. Schaefer and H.J. Pirner, Nucl. Phys. **A627** (1997) 481.
- [13] R. D. Pisarski and F. Wilczek, Phys. Rev. **D29** (1984) 338.
- [14] J. Gasser and H. Leutwyler, Phys. Lett. **B184** (1987) 83; P. Gerber and H. Leutwyler, Nucl. Phys. **B321** (1989) 387; D. Toublan, Phys. Rev. **D56** (1997) 5629.
- [15] H. J. Pirner and M. Wachs, Nucl. Phys. **A617** (1997) 395.
- [16] G. Papp, H. J. Pirner and B.-J. Schaefer, work in progress.
- [17] K.-I. Aoki et al., Progr. Theor. Phys. **99** (1998) 451.
- [18] S. B. Liao and M. Strickland, Nucl. Phys. **B532** (1998) 753.
- [19] Z. Aouissat, O. Bohr, B.-J. Schaefer and J. Wambach, work in progress.
- [20] D.-U. Jungnickel and C. Wetterich, Eur.Phys.J. **C2** (1998) 557.

- [21] C. Wetterich, Nucl. Phys. **B334** (1990) 506; *ibid.* Nucl. Phys. **B352** (1991) 529; Phys. Lett. **301B** (1993) 90.
- [22] Particle Data Group, C. Caso et al., Eur.Phys.J. **C3** (1998) 1.
- [23] R. V. Reid, Annals of Physics **50** (1968) 411.
- [24] J. J. Binney, N. J. Dowrick, A. J. Fisher and M. E. J. Newman, *The Theory of Critical Phenomena*, Oxford University Press, 1993.
- [25] R. Floreanini and R. Percacci, Phys. Lett. **356B** (1995) 205.
- [26] V. L. Eletsky and B. L. Ioffe, Sov. J. Nucl. Phys. **48** (1988) 384.
- [27] A. Gocksch, Phys. Rev. Lett. **67** (1991) 1701.
- [28] D. Ebert, Th. Feldmann and H. Reinhardt, Phys. Lett. **388B** (1996) 154.
- [29] P. Zhuang, J. Hüfner, S. P. Klevansky, Nucl. Phys. **A576** (1994) 525.
- [30] B.-J. Schaefer, Ph.D. Thesis (1997), University of Heidelberg.
- [31] H. Boschi-Filho, C. P. Natividade and C. Farina, Phys. Rev. **D45** (1992) 586.